

Responses to Editor:

We thank the Editor for a very prompt help on nominating referees, and we also appreciate the editor's thoughtful review and helpful suggestions to our manuscript. These efforts help a lot to improve the quality of our manuscript. Following are the responses to the reviewer's comments, and related revises have been incorporated into the updated manuscript.

(1). **Comment:** It would be very useful if the authors can include a tracked changes version of the re-revised manuscript in their response. It would be great if the changes made in the initial response to the two reviews and the changes made in response to these comments were tracked in different col-ours to facilitate the editing process.

Response: The tracked changes version of the manuscript is attached at the end of the authors responses file. The changes made according to the comments from 1st, 2nd, and 3rd referee, and editor are marked in purple, blue, orange, and red color, respectively. The responses provided in this document have also listed the locations of the changes made according to the comments in the manuscript (with the tracked changes version).

(2). **Comment:** In addition, what is the current status of the related and frequently cited Tong et al. paper? One can assume that the citations can at least be updated to 2016. Is it possible to state the journal to which this manuscript is submitted?

Response: The Tong et al. paper is under review at *Journal of Geophysical Research: Atmospheres*. So we have changed the citation in our manuscript as Tong et al. (2016) (see Page5Line10, 11, 25, Page6Line4, Page33Line21-23).

(3). **Comment:** Responses to reviewer 1: - Comment 4: The reviewer asks for the value of coefficient A; it can be reasonably expected other readers will also want to know this. Please include the value in the revised manuscript and not just in the review response.

Response: The value of A is added in the updated manuscript in Page5Line17.

(4). **Comment:** Responses to reviewer 1: -Comment 5 (and 3): Again, you seem not to have included anything in the paper in response to these comments, as far as I can tell (I have no tracked changes manuscript version). Please include the response to these review comments including the equation and coefficients in the revised manuscript.

Response: The response to referee 1 comment#3 and 5 is added in the updated manuscript in Page6Line17-20

(5). **Comment:** Responses to reviewer 1: -Comment 7: I cannot find the response to this comment in the revised manuscript either; please include it, in particular justification for K.

Response: The value and description of K is added in the updated manuscript in Page5Line16-17.

(6). **Comment:** Responses to reviewer 1: -Comment 8: Does equation 5 come from a

different reference? Or other justification for this equation?

Response: Equation 5 is from Marticorena et al. (1997), this has been added into the manuscript in Page6Line12.

(7). **Comment:** Responses to reviewer1: - Comment 9: In the text there is no reference to the lookup table for S_i values. Either include the table that is in the review response in the revised manuscript or include a reference to the table in a published manuscript. It also seems like here should maybe be a citation of the NAM model which the values are based on?

Response: The table for S_i values is added in the updated manuscript (Page7Line2-3, and Page35 Table1), and the reference Eric Rogers et al. (2009) is added for NAM (Page7Line3). Since a new table is added, the Table index used in the original manuscript are all revised (Page9Line13, 25, Page10Line28, Page11Line23, Page13Line1, Page17Line8, Page18Line27, Page19Line20).

(8). **Comment:** Responses to reviewer1: - Comment 10: Again I cannot find this information in the revised manuscript. Please include it.

Response: The discussion about underestimation of Ca^{2+} is added in the revised manuscript (Page15Line27-31, Page16Line1-3, 8-11).

(9). **Comment:** Responses to reviewer1: - Comment 11: The figures are still relatively hard to see. If possible, changing to a san serif font in the figures will improve readability.

Response: We have enlarged the fonts and added sub-titles in the figures. We also replaced them with .eps format for most of the figures so they can be clearly demonstrated if the manuscript is viewed in electronic version.

(10). **Comment:** Responses to reviewer 3: - Please include a sentence or two summarizing these points in the revised manuscript; in particular emphasizing the benefits of the new dust scheme given the limited improvement in agreement.

Response: The key points of the responses to reviewer 3 are focused on different questions, so we added discussions in different places in the revised manuscript to summarize these responses. The responses for comments on “does double-counting affecting other models” and “how is the improvement by correcting the double-counting issue” are summarized in Page8Line3-7. The responses for comments on “benefit of using CMAQ dust scheme” is summarized in Page8Line26-28.

(11). We would like to mention that Dr. Guoshun Zhuang at Fudan University is added as an co-author of the manuscript. Dr. Zhuang provided the local observations collected from Gobi and Taklamkan Desert, and he also helped analyze the mineralogy of dust, which is one of the key model developments implemented in this study. Dr. Zhuang analyzed the modeling results with the new dust mineralogy, reviewed the manuscript, and provided help for answering the reviewer#1’s comment#10. So after discussion with

all the other co-authors and Dr. Zhuang, we think it is proper to include Dr. Zhuang as co-author due to his contribution of this work.

Responses to Anonymous referee # 1

We thank the referee for a very thoughtful review and detailed suggestions to our manuscript. Incorporation of these suggestions helps to improve the quality of our manuscript significantly. Following are the responses to the reviewer's comments, and related revises have been incorporated into the updated manuscript.

(1). **Comment:** The main issue with the manuscript is the lack of a clear and detailed explanation of the methodology. The authors referred to the work of Tong et al. (2015) in various places in the Methodology section. This is not a published manuscript (under review in journal?) which makes it impossible for a reader to understand the details of the dust emission algorithm that the authors have used.

Response: The methodology of our study includes three major parts as described in the manuscript: first, section 2.1 introduces the development of the values of initial threshold friction velocity constant based on reanalysis of field measurement data; second, section 2.2 introduces the development of the source-dependent speciation profiles for Gobi and Taklamkan Desert; third, section 2.3 introduces the implementation of the dust heterogeneous chemistry. The reviewer's major concern is about the section 2.1. We agree with the reviewer that more details are necessary to clearly describe how the reanalysis of field data is performed, so the manuscript is revised according to this comment. Tong et al. (2016) is still under preparation to give an explicit description about the dust emission model and field measurement data. So in this manuscript, the fundamental equations and algorithms are briefly introduced. In the revised manuscript more necessary details are added to help readers to clearly understand the dust emission model (see the last paragraph of section 2.1, Page7Line25 – Page8Line20).

(2). **Comment:** It is unclear how the double-counting of the soil moisture was addressed in this study. What was the procedure for revising the original threshold velocities? It is obvious from Fig. 1(c) that the process of modifying the threshold velocities are different for different soil and land use types. What value of the soil moisture was used for each soil and land use type to modify the threshold velocities? The whole procedure needs to be presented and scientifically justified.

Response: In the original field measurements, the value of the soil moisture in each sample was provided (e.g., see Table 2 of Gillette et al., 1980). These data were used to feed the Fecan formula to derive the would-be threshold velocity under dry condition. We have reprocessed the data for the soil and land use types measured by Gillette 1980 and 1982. In case of missing data for certain soil types, we have chosen the values with the soil composition closest to a measured type following the USDA soil composition diagram (Fig 1 of Gillette et al., 1980). We have now added the information in the revised manuscript (Page7Line25 – Page8Line20).

(3). **Comment:** How (quantitatively) is the presence of non-erodible elements accounted for in calculating the threshold friction velocity and what value of the surface roughness was used?

Response: Non-erodible elements mainly include pebbles, rocks, and vegetation, while in this study only vegetation is considered. The land cover types (accompanied by soil types) determine the threshold friction velocity as calculated in Eq.(5) in section 2.1. The erodibility and roughness length used in this model only represents the potentially erodible particles such as slit, clay and sand by following the fundamental algorithm of Marticorena et al. (1997). So with this algorithm, only three land cover types are considered for erodible potential, include shrubland, mixed shrub/grassland, and barren/sparsely vegetated land. Surface roughness length (Z_{ruf}) is calculated in WRF based on vegetation fraction, while the surface roughness factor is calculated based on Z_{ruf} (see response for comment#5)

(4). **Comment:** What is the value of coefficient A (scaling factor) in Eq. (1)?

Response: The value of A is set as 32.0 in this study. The value of A is added in the manuscript (Page5Line17).

(5). **Comment:** How is the surface roughness adjusting factor ($Z_{i,j}$) calculated?

Response: The surface roughness adjusting factor Z is calculated as:

$$Z = \frac{C_1}{C_1 \times \ln Z_{ruf} - C_2}$$

The constants $C_1 = 32$ and $C_2 = -5$ used in this equation are derived from field measurement data from Gillette et al. (1980) and the relationship between roughness length and friction velocity described in Marticorena et al. (1997). This information is added in the revised manuscript (Page6Line17-20)

(6). **Comment:** The new dust speciation profiles are different for Gobi and Taklamakan. How does ONE default profile in CMAQ is replaced by these TWO profiles? Does user need to pre-define the regions where each profile is being applied?

Response: In the standard CMAQ, the default speciation profile is applied to the entire simulation domain. The two new profiles developed in this study are assigned separately to Gobi and Taklamakan based on a pre-defined map of these deserts. Yes, users need to pre-define the region where which profile should be applied.

(7). **Comment:** The vertical-to-horizontal dust flux ratio in Eq. (2) is based on the linear fitting of the measurements of Gillette (1979) by Marticorena and Bergametti (1995). The authors should note that the value of K based on this equation has the unit of [1/cm], while the rest of the formulation in the manuscript is in SI units. It seems that a factor of 100 is missed in the present calculations. Also, what would be the justification of using $K=0.0002$ for clay%>20%? Please comment.

Response: The unit of K is [1/cm] in Marticorena and Bergametti (1995) equation, and the factor 100 is implicitly reflected in the scaling factor A. The value of K (0.0002) for clay%>20% is used here following the recommendation of Marticorena and Bergametti (1995). This information is added in the revised manuscript (Page5Line16-17). We notice that this value may be subject to further changes when more measurements are made available.

(8). **Comment:** Eq. (5) is not from Fecan et. al (1999). There is no surface roughness study in their work.

Response: The reviewer is right, the Fecan et al. (1999) should be cited to support the calculation of soil moisture adjusting factor in Eq.(7), not for Eq.(5). We have correct this in the updated manuscript (Page6Line12, 17-20).

(9). **Comment:** Based on Eq. (6), the soil moisture factor is 999.9 for $S_m > W_{max}$. I think it should be the case only when $S_m > S_l$. Furthermore, the third relation should be used when $W_{max} < S_m < S_l$. Please go through the conditions in Eq. (6) and revise them. Also, how is S_l (saturation soil moisture limit) determined?

Response: The reviewer is right about the conditions in Eq.(6) (in the original version of manuscript). In fact the soil moisture S_m shall not exceed the saturation soil moisture limit S_l . We set the soil moisture adjustment factor f_{soilm} as 999.9 in the code of the model only to avoid computational abnormal values, thus it is not necessary to show this condition in the manuscript. So there are only two conditions considered, and the Eq.(6) has been revised in the manuscript as Eq.(7):

$$f_{soilm,i,j} = \begin{cases} 1.0, & \text{for } S_m \leq W_{max} \\ (1.0 + 1.21 \times (S_m - W_{max})^{0.68})^{0.5}, & \text{for } W_{max} < S_m \leq S_l \end{cases} \quad (7)$$

The value of S_l is determined based on a predefined lookup table for different landcover categories and soil types as shown below. The values in the table are mainly based on documentation of the North American Mesoscale (NAM) model. This information has been added in the revised manuscript (Page7Line2-3, Page35 Table 1)

Table Saturation soil moisture limit

Landcover Soil Type	Shrubland	Mixed shrub/grass land	Barren or sparsely vegetated
Sand	0.395	0.135	0.068
Loamy sand	0.410	0.150	0.075
Sandy loam	0.435	0.195	0.114
Silt loam	0.485	0.255	0.179
Silt	0.476	0.361	0.084
Lam	0.451	0.240	0.155
Sandy clay loam	0.420	0.255	0.175
Silty clay loam	0.477	0.322	0.218
Clay loam	0.476	0.325	0.250
Sandy clay	0.426	0.310	0.219
Silty clay	0.482	0.370	0.283
Clay	0.482	0.367	0.286

(10). **Comment:** The results deteriorate for Ca_2^+ when the new dust profile is used (Table 5). Please comment on the possible reasons.

Response: The evaluation statistics suggest that total $PM_{2.5}$ is underestimated at Duolun and Yunlin, but Ca_2^+ is overestimated under the default profile. So although the NMB value change from 36.69% by default profile to -53.12% for Ca_2^+ by revised profile, it is highly possible that the revised profile provides a better estimation of the calcium mass contribution since the evaluation statics for trace metals should be consistent with that for total $PM_{2.5}$. The overall underestimation for $PM_{2.5}$ and trace metals should be due to the underestimation of fine mode aerosol mass contribution (20%) in total dust emission. No solid conclusion is made at this point because the PM_{10} data is not available at Duolun or Yulin, although the total suspended particles (TSP) is measured and indicate the fine mode aerosol should have larger mass contribution (about 40% in TSP). This discussion has been added in the revised manuscript (Page15Line28-31, Page16Line1-3, 8-11)

(11). **Comment:** In general, the information and texts in figures are very small and hard to read.

Response: The figures are revised to make the text bigger and easier to read in the updated manuscript. Figure 1 uses larger text font, and we also reduce the number of landcover categories shown in Figure 1(a), because only three categories will generate dust in the model. Figure 2 is revised to add text indicating the locations of Fudan Univ. observational sites and TAQMN site. Figure 7 and Figure 10 has added description in the subtitles to help illustrate the information of the figures. The rest of the figures have smaller font due to limited page size, but they are all drawn as vector graphics so readers can enlarge them to have a clear view.

(12). **Comment:** Please delete the repeated word “revised” on P. 35593 line 24.

Response: It is changed in the updated manuscript (Page2Line9), thanks to the notification of the reviewer.

(13). **Comment:** In Eq. (3), the values of clay, silt, and sand should be in fraction not percentage.

Response: Yes, they should be in fraction. We have revised the text and Eq.(3) in the updated manuscript (Page5Line14-15).

(14). **Comment:** In Fig. (2), the orange rectangle (Fudan observation) and the purple diamond (TAQMN) are hard to find. Please consider marking them within the figure.

Response: Figure (2) is revised to add text and larger markers to indicate the locations of observational sites. Dr. Guoshun Zhuang from Fudan Univ. provides the data and also helps analyze the mineralogy of the dust samples collected from Taklamkan and Gobi, so he is added as an co-author in the updated manuscript (Page1Line5, 11-12).

Response to Anonymous referee # 2

We thank the referee for a very thoughtful review and detailed suggestions to our manuscript. Incorporation of these suggestions helps to improve the quality of our manuscript significantly. Following are the responses to the reviewer's comments, and related revises have been incorporated into the updated manuscript.

(1). **Comment:** The simulation period need to be clarified in the method section 2.4.

Response: The CMAQ model simulation period covers March and April from 2006 to 2010. This period is selected to represent the spring dust episode of East Asia. We have added this introduction into section 2.4 in the revised manuscript (see first paragraph of section 2.4, Page11Line11-12).

(2). **Comment:** As the analysis is mainly focused on the spring time from 2006 to 2010, it would be better to explain how to initialize the model for each year.

Response: The regional model CMAQ uses daily initial concentrations and boundary conditions provided by a global model simulation with GEOS-Chem. The downscaling method is described in Lam and Fu (2009). GEOS-Chem simulation was conducted for 5 years from 2006 to 2010. We have added this information into section 2.4 in the revised manuscript (see second paragraph of section 2.4, Page11Line15).

(3). **Comment:** Temporal coverage of observation data with screening criteria is also suggested to add in Table 4.

Response: Table 4 gives a brief introduction of the observations used in this study, and more details of these data are added into the revised manuscript in section 2.5. All the observations are collected to cover the simulation period March and April from 2006 to 2010, except for the data from Fudan Univ. network due to limited measurement efforts. The local data from Fudan Univ. has daily measurements only for 2007. We didn't apply additional screening criteria to the observations in this study because the data has already been examined before being officially release. The MODIS level2 AOD is filtered by GSFC before release. The API data is organized by China MEP and it has been screened before being published. The AERONET level 2.0 data used in this study is screened and quality assured mainly by the local agencies that organized the observational sites. The EANET data is screened and quality assured by Dr. Keiichi Sato (ksato@acap.asia) and Dr. Ayako Aoyagi (eanetdata@acap.asia) from the Asia Center for Air Pollution Research. The TAQMN data is screened and quality assured by Taiwan EPA before release.

(4). **Comment:** P35598 L17, I found difficulties to understand the function (6). Should that only apply to the case when S_m is $> W_{max}$ as stated in L11?

Response: The reviewer is right. W_{max} represents the maximum water holding capacity for each soil type. The soil moisture adjustment factor f_{soilm} is applied only when soil moisture S_m exceeds W_{max} . In addition, S_m shall not exceed the saturation soil moisture limit S_l , and the soil moisture adjustment factor f_{soilm} is set as 999.9 in the

code only to avoid computational abnormal values. So we have revised the function (6) as (see Page6Line23):

$$f_{soilm,i,j} = \begin{cases} 1.0, & \text{for } S_m \leq W_{max} \\ (1.0 + 1.21 \times (S_m - W_{max})^{0.68})^{0.5}, & \text{for } W_{max} < S_m \leq S_l \end{cases} \quad (7)$$

(5). **Comment:** P35602 L21, “the ACM2 PBL scheme” should be introduced at WRF part

Response: The reviewer is right, the WRF simulation uses ACM2 PBL scheme. The CMAQ model can define its own PBL scheme for vertical diffusion, so the vertical diffusion is configured by CMAQ again while running the. But usually the PBL schemes used by WRF and CMAQ will be the same to retain consistency. As the detailed description of the WRF configuration is described in Dong and Fu (2015a, b), we removed the description of CMAQ ACM2 PBL scheme in the revised manuscript (Page11Line6).

(6). **Comment:** P35603 L20, I would suggest to clarify that Dust_profile, Dust_Chem and Dust_Chem_High were performed based on Dust_Revised.

Response: Yes the reviewer is right, the scenario Dust_Profile, Dust_Chem, and Dust_ChemHigh are all performed based on Dust_Revised. We have added this in the revised manuscript (see last sentence of section 2.4, Page12Line1-2).

(7). **Comment:** P35605 L27, the sentence of “with relatively larger discrepancy in cities close to the Gobi Desert.” is confusing, please revise it.

Response: We intended to demonstrate that among all the cities which has API data, model evaluation results indicate relatively larger bias for those that are closer to the Gobi Desert. We realize that the original description is confusing and we have revised this sentence in the updated manuscript (Page14Line6-7).

(8). **Comment:** P35606 L1-2, is that based on daily records of all API sites from spring in 2006-2010?

Response: Yes, the evaluation statistics are calculated based on daily data pairs. We have added this information in the revised manuscript (Page14Line12-13).

(9). **Comment:** P35607 L1-2, “The two cities are close to the Gobi Desert, as shown by Fig. 1.”, Such information cannot be found in Figure 1

Response: The locations of the two cities (Duolun and Yulin) are shown in Figure 2. We have revised the description and Figure 2 in the updated manuscript (Page45).

(10). **Comment:** P35607 L19-20, need to clarify that these two observations (API and Huang et al. (2010)) cover the same time period?

Response: Huang et al. (2010) covers the period from March 20 to April 20 2007. In this study the same observation data are used to examine the simulated concentrations of trace metals and PM_{2.5} from CMAQ. The spatial distribution of modeling bias shown in Figure 3(d) is averages of March and April from 2006 to 2010. The main objective of this part is to demonstrate that CMAQ underestimates trace metals and PM_{2.5} at near desert sites (Duolun and Yulin), and meanwhile it also overestimates PM₁₀ at the near desert

area. The time period of observations is described in the updated manuscript (Page12Line28-30).

(11). **Comment:** P35608 L4-5, “O₃ (1st row), SO₂ (2nd row), SO₄²⁻ (3rd row), HNO₃ (4th row), NO_x (5th row), and NO₃⁻ (6th row)”, that doesn’t match with the layout of Figure 6

Response: In the original manuscript we submitted, Figure 6 contains 6 rows of plots in portrait direction. The edited version, after being converted into PDF format, somehow distorted the figure to cause this problem. In the revised manuscript, the description of Figure 6 is changed to remove these indications (1st row, 2nd row, 3rd row, 4th row, 5th row, 6th row) because the figures are self-explained by the captions (Page52).

(12). **Comment:** P35609 L10-12, “The elevation of NO_x concentration should be attributed to the conversion of gas-phase HNO₃ back to NO_x (Yarwood et al., 2005)” Since O₃ and OH is reduced, that might also account for the change in NO_x and NO₃

Response: The reviewer is right, we have add this in the discussion (Page17Line31).

(13). **Comment:** P35635 Figure 2, the orange rectangles are hardly to find. It would be helpful to add the location of the Gobi and Taklamakan desert as well.

Response: The approximate area of Gobi and Taklamakan desert is marked in the revised figure. The location of orange rectangles are also revised to make them easier to be found (Page45).

(14). **Comment:** P35596 L3, “simulation” to “simulations”

Response: This is revised according to the reviewer’s comment in the updated manuscript (Page4Line11).

(15). **Comment:** P35597 L20, “elsewhere” to “in”

Response: This is revised according to the reviewer’s comment in the updated manuscript (Page5Line24).

(16). **Comment:** P35599 L23, “emission” to “emissions”

Response: This is revised according to the reviewer’s comment in the updated manuscript (Page8Line12).

(17). **Comment:** P35606 L4, “simulation without dust emission” to “no dust emissions”

Response: This is revised according to the reviewer’s comment in the updated manuscript (Page14Line15-16).

(18). **Comment:** P35607 L15, “one set of data pairs” to “Dust_Profile”

Response: This is revised according to the reviewer’s comment in the updated manuscript (Page15Line25).

(19). **Comment:** P35614 L28, “al” to “all”

Response: This has been revised according to the reviewer's comment in the updated manuscript (Page23Line12).

(20). **Comment:** P35615 L19, "comapred" to "compared"

Response: This sentence has been revised according to the reviewer's comment in the updated manuscript (Page24Line4-6).

(21). **Comment:** P35617 L7, "Model development" to "Dust model"

Response: This has been revised according to the reviewer's comment in the updated manuscript (Page25Line27-28).

(22). **Comment:** P35617 L16, "bye" to "by"

Response: This has been revised according to the reviewer's comment in the updated manuscript (Page26Line6).

(23). **Comment:** P35628 Table 1, "in next section" to "in this study"

Response: This sentence has been deleted in the updated manuscript since we realize it is redundant (Page36Line2-3).

(24). **Comment:** P35630 Table 3, "intial" to "initial"

Response: This has been corrected (Page40).

(25). **Comment:** P35631 Table 4, please check the title

Response: The title of Table 4 (Table 5 in the revised manuscript) has been changed to "Observations used in this study" (Page5).

Response to Anonymous referee # 3

We thank the referee for a very thoughtful review and detailed suggestions to our manuscript. Incorporation of these suggestions helps to improve the quality of our manuscript significantly. Following are the responses to the reviewer's comments, and related revises have been incorporated into the updated manuscript.

(1). **Comment:** An important issue is that the Tong et al. paper detailing the dust scheme used in this study is currently not published. Perhaps it has been accepted since submission, but without that manuscript in the literature first it is difficult to see how this work can be published. There are many details left out of the description of the dust scheme, probably because they are explained in Tong et al., which is all the more reason to wait to publish once that has been peer-reviewed.

Response: The dust scheme used in the standard version of CMAQ and this study is the same, and the developments implemented in this study are all based on the standard version of CMAQ with FENGSHA dust scheme. FENGSHA is developed by Dr. Daniel Tong with his co-authors, and we are also expecting to see the publication of Tong et al., 2015. We agree that with the publication of Tong et al. may provide a more comprehensive description of the dust emission scheme. But the fundamental functions and algorithms are described clearly in our manuscript, and we also include more details about how the parameterization of friction velocity is improved in this study in the revised manuscript. So our updated manuscript can also provide a clear description of the scheme to make it easy to be understood. The major objective of our manuscript is to demonstrate how the improvements employed in this study can result in better performance of the original scheme in CMAQ, and also point out the potential remaining issues within it. Thus a fully explicit description of the original scheme is beyond our focus. In fact, a few publications (Appel et al., 2013; Fu et al., 2014) have already investigated the CMAQ model performance with FENGSHA scheme since the first release (CMAQv5.0 released in 2012), while our manuscript is the first one that provide detailed description of the functions and parameters. With the newly added information, the updated manuscript now provides a clear introduction of the scheme now.

(2). **Comment:** The work of Wang et al. (2012) implements two established dust schemes into the CMAQ model, including heterogeneous chemistry, and evaluates them over Asia. This paper is mentioned in the manuscript, but it would be valuable to provide a comparison because the baseline version of CMAQ performs so poorly when simulating Asian dust, and therefore most changes would improve upon the baseline. For example, what benefit does the FENGSHA dust scheme bring that justifies including it, rather than one of the more established dust schemes? I think the heterogeneous source mineralogy profiles are an improvement over the Wang et al. (2012) study, although the improvement in agreement with observations (shown in Figure 5 and Table 5) appears limited.

Response: Our study focused on how to improve the FENGSHA scheme within the standard CMAQ model. We point out that the poor performance of baseline CMAQ was

mainly due to the overestimation of threshold friction velocity, which is attributed to the double-count of soil moisture effect in the original parameterization. The dust scheme used in our study is different from the two used by Wang et al., (2012) in terms of the microphysical parameterization. Wang implemented two schemes, the Westphal scheme and the Zender scheme, both of which are well-established. We did not include detailed comparison between our work and Wang's work mainly for two reasons: First, the FENGSHA is developed by Tong et al. and adopted by U.S. EPA for the standard CMAQ version, our study is focused on the CMAQ model application and improvement. While the developments implemented by Wang et al. (2012) was not public available, we are unable to examine their model performance for our case study; Second, in our study, dust is speciated into 19 sub-species to make it compatible with the aerosol-related schemes within CMAQ modeling system, while Wang's work treated dust as a unique independent species. Thus comparing the work by Wang et al. (2012) is inapplicable and beyond the focus of our study. The reviewer raised a very interesting question about the benefit of FENGSHA as compared to other schemes. The most important specialty that distinguish FENGSHA from all other scheme is that it speciates dust emission into sub-aerosol species, while conventional schemes mostly treat dust as a unique species in the model. But without carefully designed schemes comparison study, it remains an open-ended question that how FENGSHA can benefit the model with better performance. This information has been added briefly in the revised manuscript (Page8Line26-28).

(2). **Comment:** Do the authors think that the assumption that the Gillette et al. field data is for zero soil moisture conditions will be a factor for other dust schemes? If so this perhaps needs pointing out.

Response: The Gillette et al. (1980) data affects the FENGSHA scheme because the parameterization rely on initial threshold friction velocity which are influenced by the soil moisture. The double-count of soil moisture effect occurred when Tong et al developed the FENGSHA scheme, thus the discrepancy is not related with the Gillette data. Although other schemes (such as the Westphal scheme) may also consider the impact of soil moisture, their parameterization methods are different and use independent field campaign data. So for our knowledge we donot think there is any well-established dust emission scheme may has the same issue as discussed in our study. This information has been added briefly in the revised manuscript (Page8Line3-7)

(3). **Comment:** Can the authors test the emissions and the agreement with observations using the GLDAS soil moisture data set shown in Figure 10? The authors state that there is no observational data between 2006-2010 over East Asia, but testing the GLDAS soil moisture seems like a relatively trivial test that would provide an answer to the open question of whether soil moisture explains the underestimate of emissions in the Taklamakan.

Response: We did not perform simulation with the GLDAS reanalysis data in this study since it doesn't provide all the required variables for WRF simulation. GLDAS v2 data has

22 variables (<http://hydro1.sci.gsfc.nasa.gov/data/s4pa/GLDAS/README.GLDAS2.pdf>) while the FNL ds083.2 data contains 116 variables (<http://rda.ucar.edu/datasets/ds083.0/>). We do plan to use the GLDAS soil moisture and soil temperature data only with other inputs from FNL to perform test simulation, but this is not a trivial work if considering the inconsistency between GLDAS as an assimilation data and FNL as a reanalysis data. In addition, even GLDAS may drive model prediction (such as results shown in Haustein et al., 2013) closer towards observations, but it may not necessarily demonstrate the better quality of GLDAS, so we are looking for soil moisture observation data to address this issue.

(4). **Comment:** pg 35593 ln 5 - the talk of double-counting feels too specific for the abstract, unless the soil moisture issue is a general issue that the authors wish to bring to the attention of the community. ln24 - "revised" repeated.

Response: We emphasize the double-counting in the "Abstract" section because this is the major factor that responsible for the underestimation of dust emission by the standard CMAQ model. As the previous model applications found out the underestimation issue but couldn't address the reason, it is necessary to clearly state it to help the research community realize and correct it in the modeling system. The repeated "revised" has been removed in the updated manuscript (Page2Line9).

(5). **Comment:** pg 35595 ln8 - "deposition".

Response: Thanks to the reviewer's comment, this sentence has been changed to "deposition and surface concentration" in the updated manuscript (Page3Line18).

(6). **Comment:** pg 35599 ln 16 'soil moisture' ln 28 - diameter or radius?

Response: When describing size bins of aerosols model usually refers aerodynamic diameter, so we did not specifically mention it in the manuscript.

(7). **Comment:** pg35607 ln2 - I can't see the two cities on Figure 1

Response: That was a typo, the locations of the two cities are added in Figure 2 in the updated manuscript, and description in the text is also revised (Page45).

(8). **Comment:** pg 35615 ln 1 - is the slightly increasing trend significant or not?

Response: Dust emission is predominantly determined by the wind field which may vary from year to year as a result of the regional climate change. So with the only 5 springs in this study we are hesitate to reach solid conclusion regarding if the trend is significant or not, because longer term investigation is necessary to answer this question. But based on both the observations and model simulations, the year 2010 showed higher dust emission than 2006 due to the severe drought over East Asia. In the manuscript we mentioned the slightly increasing trend of dust to demonstrate that modeling bias of PM10 is affected by the simulation of dust emission. This information has been added briefly in the revised manuscript (Page25Line16-17).

(9). **Comment:** pg 35616 ln 21 - 'aerosols' ln 23 - how close are Duolun and Yulin to source? The sedimentation of coarse particles will alter PM_{2.5}/TSP with distance, do you take this into account?

Response: The locations of Duolun and Yulin are marked in Figure 2 in the updated manuscript. Duolun is at the east edge, and Yulin is close to the southeast edge of Gobi Desert, so both of them are quite close to the source area. As coarse particles deposit faster than fine particles, the ratio of PM_{2.5}/TSP at these two cities should be higher than that in the middle of the Gobi Desert. But unfortunately that's the only two sampling sites we can find that provide observation data, so we did not make solid conclusion about the PM_{2.5}/PM₁₀ ratio in the CMAQ model. And this is also the reason that we recommend the research community to devote more efforts to look into this uncertainty in the modeling system (Page16Line8-12).

(10). **Comment:** pg 35617 ln7 - rephrase this, implementing development doesn't really describe anything.

Response: We also realize that the original manuscript needs to be rephrased to get better quality. In the updated manuscript, the sentence has been revised as: "The dust module in CMAQ has been further developed in this study." (Page25Line27-28).

(10). **Comment:** Figure and table captions could do with improving and cross-referencing. e.g. Table 5 does not mention what the model is evaluated against and should reference Table 4 for this, at least. Figure 3 doesn't include the time frame for the data comparison. Figure 5 should either include the statistics or the caption reference Table 5.

Response: This is a very helpful comment and we appreciate it. In the updated manuscript, caption of Figure 3 is revised to indicate the time as "five-year average"; caption of Figure 5 is revised to reference Table 5 and Table 6.

(11). **Comment:** References Wang, K., Zhang, Y., Nenes, A. and Fountoukis, C.: Implementation of dust emission and chemistry into the Community Multiscale Air Quality modeling system and initial application to an Asian dust storm episode, Atmos. Chem. Phys., 12(21), 10209–10237, doi:10.5194/acp-12-10209-2012, 2012.

Response: The DOI number of the reference has been added in the updated manuscript (Page33Line31).

Model development of dust emission and heterogeneous chemistry within the Community Multiscale Air Quality modeling system and its application over East Asia

Xinyi Dong¹, Joshua S. Fu^{1,2}, Kan Huang¹, Daniel Tong^{3,4,5}, [Guoshun Zhuang⁶](#)

¹Department of Civil and Environmental Engineering, the University of Tennessee, Knoxville, TN 37996, USA

²Climate Change Science Institute, Oak Ridge National Laboratory, Oak Ridge, TN 37831, USA

³NOAA/OAR/ARL, NOAA Center for Weather and Climate Prediction, College Park, MD 20740, USA

⁴Center for Spatial Information Science and Systems, George Mason University, Fairfax VA 22030, USA

⁵Cooperative Institute for Climate and Satellites, University of Maryland, College Park, MD 20740, USA

⁶[Center for Atmospheric Chemistry Study, Department of Environmental Science and Engineering, Fudan University, Shanghai 200433, China](#)

* Correspondence to: Joshua S. Fu (jsfu@utk.edu)

Abstract

The Community Multiscale Air Quality (CMAQ) model has been further developed in terms of simulating natural wind-blown dust in this study, with a series of modifications aimed at improving the model's capability to predict the emission, transport, and chemical reactions of dust. The default parameterization of initial threshold friction velocity constants ~~in the CMAQ~~ are revised to ~~avoid correct the~~ double counting of the impact of soil moisture in CMAQ by re-analysis of field experiment data; source-dependent speciation profiles for dust emission are derived based on local measurements for the Gobi and Taklamakan deserts in East Asia; and dust heterogeneous chemistry is also implemented. The improved dust module in the CMAQ is applied over East Asia for March and April from 2006 to 2010. Model evaluation result shows that the simulation

bias of PM_{10} and aerosol optical depth (AOD) is reduced from -55.42% and -31.97% by the original CMAQ to -16.05% and -22.1% by the revised CMAQ, respectively. Comparison with observations at the nearby Gobi stations of Duolun and Yulin indicates that applying a source-dependent profile helps reduce simulation bias for trace metals. Implementing heterogeneous chemistry also results in better agreement with observations for sulfur dioxide (SO_2), sulfate (SO_4^{2-}), nitric acid (HNO_3), nitrous oxides (NO_x), and nitrate (NO_3^-). Investigation of a severe dust storm episode from 19 to 21 March 2010 suggests that the revised CMAQ is capable of capturing the spatial distribution and temporal variation of dust. Model evaluation also indicates potential uncertainty within the excessive soil moisture used by meteorological simulation. The mass contribution of fine mode particles in dust emission may be underestimated by 50%. The revised-revised CMAQ model provides a useful tool for future studies to investigate the emission, transport, and impact of wind-blown dust over East Asia and elsewhere.

1. Introduction

Natural dust has a wide impact on many different aspects of the Earth's system. It reduces atmospheric visibility (Engelstaedter et al., 2003; Kurosaki and Mikami, 2005; Washington et al., 2003), deteriorates air quality (De Longueville et al., 2010; Prospero, 1999), alters the radiative forcing budget (Liao et al., 2004; Miller et al., 2006; Reddy et al., 2005), and also affects the cloud properties and precipitation (Rosenfeld et al., 2001; Forster et al., 2007). Over East Asia, spring time dust storms often lead to severe air pollution since the intensively elevated aerosol loadings are dumped over the most populated areas. The estimated global source of mineral dust with diameters below $10\mu m$ is between 1,000 and 4,000 Tg/year on a global scale as reported by Intergovernmental Panel on Climate Change (IPCC), and Zhang et al. (2003) reported annual Asian dust emission as 800 Tg. East Asian dust mainly originates from two dominant source regions and their surrounding areas, including the Taklamakan Desert in northwest China and the Gobi Desert in Mongolia and northern China (Huang et al., 2010). In spring, the Mongolian Cyclone associated with the East Asian trough often leads to strong northwesterly near surface winds (Shao and Dong, 2006) that lift and transport the eolia

dust particles. East Asian dust can transport to densely populated areas over China (Qian et al., 2002), South Korea (Chun et al., 2001; Park and In, 2003), and Japan (Ma et al., 2001; Uno et al., 2001), and at times can even transport across the Pacific Ocean, reaching as far as the west coast of North America (Fairlie et al., 2010; Wang et al., 2012; Zhao et al., 2010). Along the transport pathway, mineral dust particles also serve as carriers and reaction platforms by uptaking reactive gases such as ozone (O_3), nitrogen oxides (NO_x), sulfur dioxide (SO_2), nitric acid (HNO_3), hydroxyl radicals (OH), and volatile organic compounds (VOCs). The dust heterogeneous chemistry may change the photochemistry, acid deposition, and production of secondary aerosols in the atmosphere. Besides, East Asian dust is believed to contribute geochemically significant amounts of minerals that are deposited into the western part of the Pacific Ocean. These minerals may alter the oceanic primary productivity (Zhang et al., 2003; Zhuang et al., 1992) as well.

Since natural dust links the biogeochemical cycle of land, atmosphere, and ocean, understanding the emission, evolution, and transport of dust is essential for further examining its impacts on the Earth's system. Numerical modeling is one of the most important approaches for systematically investigating dust. Many global models simulate dust emissions, transport, and depositions. Huneus et al. (2011) conducted intercomparisons of 15 global models and reported their simulated aerosol optical depth (AOD) and Angström Exponent (AE) within a factor of two and the ~~total~~ deposition and surface concentration within a factor of 10 with respect to observations, indicating significant variations among different models. Regional models usually represent dust by following a coherent manner as global models. For example, the WRF-Chem (Grell et al., 2005) coupled with the GOCART scheme (Ginoux et al., 2001) has been applied to simulate dust emission over Middle-East Asia (Kumar et al., 2014), the United States (Zhao et al., 2010), and East Asia (Chen et al., 2013). The STEM (Carmichael et al., 2003) used the COAMPS scheme (Liu and Westphal, 2001) and has been applied over East Asia (Tang et al., 2004). Regional models have fine spatiotemporal resolution and multiple physical parameterizations at the cost of intensive computation. As compared to global models, regional models may provide more realistic representations of the surface

roughness, soil moisture and contents, and also allow comparable validation against surface observations (Darmenova and Sokolik, 2008).

The Community Multiscale Air Quality (CMAQ) model is a state-of-science model and has been applied in numerous regional modeling studies worldwide. Unlike other models in which dust is usually treated as a unique aerosol, the CMAQ distributes dust particles into 19 aerosol species, such as inorganic aerosols and trace metals. This approach is consistent with the original design of the CMAQ as an air quality model, and it also provides a potential platform to examine the diversities of chemical and physical properties within dust particles. It enables the model to examine the mixing status and net effect of natural dust and anthropogenic aerosols on air quality and regional climate. The validation of the CMAQ performance is not well understood due to limited research efforts. Appel et al. (2013) conducted a full year simulation with CMAQ over the continental United States for 2006, and reported good agreement between simulation and observations, with the mean bias around $\pm 0.5 \mu\text{g}/\text{m}^3$ and $0.5\text{-}1.5 \mu\text{g}/\text{m}^3$ ($\sim \pm 30\%$) for soil concentrations over western and eastern United States, respectively. But the CMAQ simulations over other regions underestimate dust emissions significantly. Fu et al. (2014) reported that the default dust scheme in the CMAQ underestimated dust emission by 98% during a six-day dust storm episode in 2011. With the modeling domain covering the entire Northern Hemisphere, Xing et al. (2015) also suggested that the CMAQ underestimated AOD by 30%-60% in areas where dust is dominant, while the bias was less than $\pm 15\%$ elsewhere.

The studies mentioned above indicate that the capability of the CMAQ for simulating natural dust emissions remains poorly understood. In addition, the current dust scheme in the CMAQ does not include dust heterogeneous chemistry, while some studies have revealed the important impact of dust chemistry on ambient air pollutants with both measurement (Krueger et al., 2004; Matsuki et al., 2005; Usher et al., 2003) and modeling evidence (Bauer et al., 2004; Bian and Zender, 2003; Dentener et al., 1996). The objective of this study is to evaluate and improve the model's capability of reproducing dust emission, and also enable the model to treat the dust heterogeneous chemistry. Section 2 introduces the method of applying new parameterizations and implementing dust heterogeneous chemistry into the CMAQ, whereas Section 3

summarizes the improved model performance. Section 4 discusses the enhanced model capability and remaining uncertainties, and Section 5 concludes the paper with a summary of the findings.

2. Methodology

2.1 Improvement of the CMAQ wind-blown dust emission module

The process of wind-blown dust emission is controlled by a number of environmental variables, including wind speed, soil texture, land use type, vegetation cover, and soil moisture. Dust deflation is favored by dry soil with low and sparse vegetation and constrained by high soil moisture. The dust emission scheme employed in the CMAQ is developed by Tong et al. (2016). The emission (vertical flux) of the dust F (g/m²s) was estimated based on a modified Owen's equation (Owen et al., 1964; Tong et al., 2016):

$$F = \sum_{i=1}^M \sum_{j=1}^N K \times A \times \frac{\rho}{g} \times S_i \times SEP \times u_* \times (u_*^2 - u_{*ti,j}^2) \quad \text{for } u_* > u_{*ti,j} \quad (1)$$

where M is the erodible land use type, N is the soil texture type, K is the ratio of vertical to horizontal flux calculated based on the amount of clay (*clay%*) within the soil:

$$K = \begin{cases} 10^{0.134 \times (\text{clay}\%) - 6}, & \text{when : } \text{clay}\% < 20\% \\ 0.0002, & \text{when : } \text{clay}\% \geq 20\% \end{cases} \quad (2)$$

The value of K (0.0002) for $\text{clay}\% > 20\%$ is used here following the recommendation of Marticorena and Bergametti (1995). A is a scaling factor (set as 32.0 in this study), ρ is air density, g is gravitational acceleration (9.8 m/s²), S_i is dust source area for land type i , SEP is the soil erodibility factor, which is calculated based on the amount-fraction of clay, silt, and sand of the soil as:

$$SEP = 0.08 \times \text{clay} + 1.0 \times \text{silt} + 0.12 \times \text{sand} \quad (3)$$

$$\text{SEP} = 0.08 \times \text{clay}\% + 1.0 \times \text{silt}\% + 0.12 \times \text{sand}\%$$

(3)

u_* is the friction velocity, and $u_{*ti,j}$ is the threshold friction velocity for soil type j and land use type i . More details of the dust emission algorithm have been given elsewhere in

(Tong et al., 2016). Equation (1) is applied only when the model calculated friction velocity exceeds the designated threshold value. Therefore, the value of threshold friction velocity is critical to determine the onset and magnitude of dust emission in the CMAQ model.

In the CMAQ dust module, the threshold friction velocity is dynamically calculated based on the presence of non-erodible elements and the change of soil moisture (Tong et al., 2016). The effect of non-erodible elements is represented by wind energy partitioning following Marticorena et al. (1997). The effect of soil moisture on dust emission is implemented following a two-step approach proposed by Fecan et al. (1999). First, the maximum water holding capacity (W_{max}) for each soil type is determined based on the amount of clay in the soil:

$$W_{max} = (0.0014 \times clay + 0.17) \times clay \quad (4)$$

In case that soil moisture exceeds W_{max} , the threshold friction velocity is then adjusted (Marticorena et al., 1997) using a revised Fecan formulation (Fecan et al., 1999) as:

$$u_{*i,j} = u_{*ci,j} \times Z_{i,j} \times f_{soilm\ i,j} \quad (5)$$

where $u_{*ci,j}$ is the initial threshold friction velocity constant, $Z_{i,j}$ is the surface roughness adjusting factor calculated with surface roughness length from the meteorology field, calculated as:

$$Z = \frac{C_1}{C_1 \times \ln Z_{ruf} - C_2} \quad (6)$$

The constants $C_1 = 32$ and $C_2 = -5$ used in this equation are derived from field measurement data from Gillette et al. (1980) and the relationship between roughness length and friction velocity described in Marticorena et al. (1997).

And $f_{soilm\ i,j}$ is the moisture adjustment factor calculated using a revised Fecan formulation (Fecan et al., 1999) as:

$$f_{soilm\ i,j} = \begin{cases} 1.0, & \text{for } S_m \leq W_{max} \\ \left(1.0 + 1.21 \times (S_m - W_{max})^{0.68}\right)^{0.5}, & \text{for } W_{max} < S_m \leq S_l \end{cases} \quad (7)$$

$$f_{soilm\ i,j} = \begin{cases} 999.9, & \text{for } S_m > W_{max} \\ 1.0, & \text{for } S_m \leq W_{max} \\ \left(1.0 + 1.21 \times (S_m - W_{max})^{0.68}\right)^{0.5}, & \text{for } S_m \leq S_l \end{cases} \quad (6)$$

where S_m is soil moisture, and S_l is the saturation soil moisture limit determined by soil textures. The values of S_l are given by the North American Mesoscale (NAM) modeling system (Rogers et al., 2009), as summarized in Table 1.

Previously, the values of initial threshold friction velocity constant were taken from observed data from wind tunnel experiments conducted by Gillette and co-workers (Gillette et al., 1980, 1982). Fu et al. (2014) reported the $u_{*ci,j}$ used in the CMAQ has an average value of 0.7m/s among all soil types, which is too high to generate enough dust particles over East Asia. Fu et al. (2014) used a fixed value of 0.3m/s based on a study of local measurements in a northern desert in China (Li et al., 2007). Although this smaller threshold helps ~~to~~ generate higher production of dust emission during the six-day simulation episode from 1 to 6 May 2011, the arbitrarily designated threshold value for all land covers and soil categories prevents the model from reproducing spatial and temporal variations of dust emission. In this study, We have conducted a reanalysis of the ~~Gillette~~-field data (Gillette et al., 1980, 1982) and revised the threshold friction velocities through removing the double counting of soil moisture in the CMAQ dust emission modeling. In these field campaigns, While some of these experiments were performed under rather dry conditions, but for ~~most of the~~other samples the effect of soil moisture ~~effect~~ cannot be ignored. Therefore, these values reported from field experiments are not always suitable ~~to be~~for being used directly as the initial threshold friction velocity constant, which is assumed to represent extremely dry conditions. Meanwhile, in the CMAQ dust module, dynamic soil moisture data are used to adjust threshold friction velocity. Therefore, we need to convert the wet-condition data into threshold values under dry conditions. Otherwise, there will be double counting of soil moistures under some cases.

We took a three-step approach to calibrate the threshold friction velocity. First, the value of soil moisture was extracted for each sample from the raw field dataset (courtesy from

1 Dale Gillette, retired). Next, these data were used to feed the Fecan formula (Fecan et al.
 2 1999) to derive the dry-condition threshold velocity by casting soil moisture back to zero.
 3 We have reprocessed the data for the soil and land use types measured by Gillette 1980
 4 and 1982. In case of missing data for certain soil types, we have chosen the values with
 5 the soil composition closest to a measured type following the USDA soil composition
 6 diagram (Fig 1 of Gillette 1980). Finally,~~In this study,~~ the revised values of $u_{*ci,j}$ are
 7 implemented into the CMAQ. For our knowledge the double-counting issue affects the
 8 dust emission module in CMAQ only because the microphysical parameterization is
 9 developed based on Gillette et al. (1980) data. It also explains the significant
 10 underestimations of dusty by CMAQ as reported in Apple et al. (2013) and Fu et al.
 11 (2014). Comparison of the default and revised constants are summarized in Figure 1 (c).
 12 As the double-count of soil moisture has been corrected, the revised constants are lower
 13 than the default ones. The majority of land cover in the Gobi is categorized as shrub land,
 14 where the revised initial threshold friction velocity constants are significantly lower than
 15 the default values for all soil types as shown in Fig. 1 (c), indicating that the revised
 16 scheme is expected to produce higher dust emissions over the Gobi. The Taklamakan
 17 Desert is mainly configured as barren or sparsely vegetated land cover with sandy soil
 18 type, which only shows a small drop of the threshold friction velocity constant from
 19 0.28m/s to 0.23m/s, indicating that the changes of dust emission over the Taklamakan
 20 may not be substantial. The CMAQ distributes dust emission to four size bins: 0.1-1.0 μ m,
 21 1.0-2.5 μ m, 2.5-5.0 μ m, and 5.0-10.0 μ m with the mass contribution as 3%, 17%, 41%, and
 22 39% within each bin, respectively. The first two bins represent the fine mode aerosol and
 23 the larger two represent the coarse mode. So the mass contribution is 20% for fine mode
 24 80% for coarse mode aerosol.

25 **2.2 Implementing source-dependent speciation profile**

26 The emission of natural wind-blown dust particles is distributed to 19 aerosol species in
 27 the CMAQ following the profile developed based on the EPA's SPECIATE database
 28 (Simon et al., 2010). As compared with other models that treat dust as a unique aerosol
 29 species, the CMAQ approach provides a more detailed description of ~~the chemical~~
 30 ~~components of dust~~ dust mineralogy. This feature benefits CMAQ by enabling the model

to maintain the consistency between dust and other types of existing aerosol in the modeling system. However, mass contributions of different chemical components may

differ greatly among different source areas, thus using a fixed profile for all dust sources may introduce uncertainty and lose the capacity of modeling the varieties of dust particles. The mass contribution of Aluminum (*Al*) is around 5%~8% for pure minerals around the world, and the ratios between other trace metals and *Al* may vary substantially for different dust particles. Thus the elemental mass ratio between Calcium and Aluminum (*Ca/Al*) is usually used to identify the source of dust samples (Huang et al., 2010; Sun et al., 2005). For example, the *Ca/Al* ratio for Saharan dust is around 0.9 and 1.0 for fine and coarse dust particles, respectively (Blanco et al., 2003; Formenti et al., 2003; Kandler et al., 2007; Reid et al., 2003); for Arabian dust is around 0.13 and 0.15 for coastal and inland dust, respectively (Krueger et al., 2004); for Taklamakan dust is about 1.5~1.9 (Huang et al., 2010); and for dust from the Gobi Desert is 0.4~1.1 (Arimoto et al., 2006; Zhang et al., 2003). To characterize the dust aerosols in the CMAQ better, source-dependent speciation profiles are developed in this study for the Gobi and Taklamakan deserts based on local measurement data collected by Huang et al. (2010).

These two profiles are compared with the default one in the CMAQ as shown in Table 42. For the model species which are not measured in Huang et al. (2010), including primary organic carbons (APOC), non-carbon aerosols (APNCOM), elementary carbons (EC), silicon (ASI), and water (AH2O), their values for the Taklamakan and Gobi are kept the same as in the default profile. And for unspiciated (AOTHR) and non-anion dust (ASOIL), their values in the two new profiles are calculated based on the contributions of all other species, to keep the total mass contributions conservative. It is important to notice that the model species refer to an anion or cation phase for sulfate (ASO4, SO_4^{2-}), nitrate (ANO3, NO_3^-), chloride (ACL, Cl^-), ammonium (ANH4, NH_4^+), sodium (ANA, Na^+), Ca_2^+ (ACA), magnesium (AMG, Mg_2^+), and potassium (AK, K^+), and an element phase for iron (AFE, *Fe*), *Al*(AAL), silicon (ASI, *Si*), titanium (ATI, *Ti*), and manganese (AMN, *Mn*). Mass contributions of different aerosols differ significantly among the profiles as shown in Table 42. For example, Ca_2^+ accounts for 7.94% of the total fine particle mass in the default profile, which is much higher than the Taklamakan (2.063%) and the Gobi (1.788%). For Mg_2^+ , the default profile assumes a zero

percentage of mass contribution, yet the values for the Taklamakan and Gobi are 0.165% and 0.799%, respectively. The K^+ contribution within the default profile is 3.77%, while the Taklamakan is 0.153% and the Gobi is 0.282%. Si is one of the most abundant metals in the crust, yet the default speciation profile has an inappropriate assumption as zero Si content in coarse mode dust particles. As no measurements are found for Si over the Taklamakan or Gobi, we use the element ratio of Al/Si as 8%/28% to derive the mass contribution of Si in the coarse model, which is a conventional approach for trace metal analysis (Huang et al., 2010). Different configurations within the speciation profile will lead to significant differences of model predictions for these trace metals, demonstrated in more detail in Section 3.

2.3 Implementation of heterogeneous reactions

The default heterogeneous chemistry scheme within the CMAQ considered the conversions from N_2O_5 to HNO_3 , and from NO_2 to $HONO$ and HNO_3 . These reactions play an important role in the nighttime production of nitrate aerosols (Dong et al., 2014; Pathak et al., 2011; Pun and Seigneur, 2001). Heterogeneous reactions are treated as irreversible in the model (Davis et al., 2008; Sarwar et al., 2008; Vogel et al., 2003). While dust particles serve as a platform for heterogeneous reaction, they also participate in some of the reactions to uptake the gas-phase species. The uptake of gases onto the surface of dust particles is defined by a pseudo-first-order reaction rate K (Dentener et al., 1996; Heikes and Thompson, 1983) calculated as:

$$K = \left(\frac{r_p}{D_g} + \frac{4}{v_g \gamma_g} \right)^{-1} A_p \quad (8)$$

where r_p is the radius of the particle, D_g is the diffusion coefficient of gas molecules, v_g is the mean molecular velocity of gas, A_p is the surface area of the particle, and γ_g is the uptake coefficient for gas. Many research efforts have been devoted to quantify the uptake coefficients. The reported values of the uptake coefficient may differ by more than 2-3 orders of magnitude, depending on the source of the dust samples and analytical methods (Cwiertny et al., 2008; Usher et al., 2003). While this work focuses on East Asia, the uptake coefficients are mainly collected from Zhu et al. (2010), which summarized

the estimations for dust samples from deserts in China. The "best guess" of uptake coefficients were suggested based on the analysis of different measurement studies summarized in Zhu et al. (2010). But in this study both the lower and upper limits of uptake coefficients are examined to evaluate their impacts. Table 2-3 lists the 13 dust heterogeneous reactions implemented into the CMAQ in this study, with the lower and upper boundaries of uptake coefficients.

2.4 Model inputs, configuration, and simulation scenarios

The CMAQ model simulation uses version 5.0.1. In this study, the CMAQ is configured with the updated 2005 carbon bond gas-phase mechanism (CB05), aerosol module AE6, in-line photolysis calculation and NO emission from lightning, ~~the ACM2 PBL scheme,~~ and the Euler backward iterative (EBI) solver. The modeling domain covers East Asia and Peninsular Southeast Asia as shown in Figure 2. The CMAQ simulation is performed with a 36km horizontal grid spacing and 34 vertical layers with a model top as 50hPa, with finer resolution at the near surface layers to represent clearly the planetary boundary layer. Simulation period covers March and April from 2006 to 2010 to represent the spring dust episode of East Asia.

The meteorology field is simulated with the Weather Research and Forecasting model (WRFv3.4, Skamarock et al., 2008). Initial and boundary conditions are generated downscaled from the GEOS-Chem global model simulation for 2006-2010 by following the routines described in Lam and Fu (2009). Biogenic emission is from MEGAN2.1 (Guenther et al., 2006; Muller et al., 2008), biomass burning emission is from FLAMBE (Reid et al., 2009), and anthropogenic emission is from Zhao et al. (2013) over China and INTEx-B over other countries within the domain. More details about meteorology and emission datasets are described in Dong and Fu (2015a, b).

To examine the performance of the CMAQ model development with revised parameterization and dust heterogeneous reactions, a total of six scenarios are conducted as listed in Table 34. The simulations Dust_Off and Dust_Default are designed to investigate performance of the CMAQ without dust emission and with the default dust plume rise scheme; Dust_Revised is designed to investigate the performance of applying the new parameterization of initial friction velocity threshold constants; Dust_Profile is

designed to examine the improvement by applying source-dependent dust composition profiles; and Dust_Chem and Dust_ChemHigh are designed to examine the impacts of implementing heterogeneous chemistry with lower and upper estimations of uptake coefficients, respectively. [The scenario Dust Profile, Dust_Chem, and Dust_ChemHigh are all performed based on Dust Revised.](#)

2.5 Observations

Both ground-based measurements and satellite observations are used in this study to help examine the uncertainty and evaluate the performance of the model. The Air Pollution Index (API, <http://datacenter.mep.gov.cn>) reported by the Chinese Ministry of Environmental Protection (MEP) is used to evaluate the PM₁₀ predictions from the CMAQ. The API is reported on a daily basis with a national coverage of 86 middle size or larger cities in China and has been applied in many modeling studies for evaluation purposes (Zhao et al., 2013). To investigate the transport of dust particles over downwind areas simulated by the model, we also used surface observations from the Acid Deposition Monitoring Network in East Asia (EANET; EANET, 2007) over Japan, and observations from the Taiwan Air Quality Monitoring Network (TAQMN; <http://taqm.epa.gov.tw/taqm/en/default.aspx>). EANET provides hourly or daily records of PM₁₀, O₃, NO_x, and SO₂, and also bi-weekly (or longer interval) records of HNO₃, SO₄²⁻, and NO₃⁻. Data from EANET is also employed in this study for examining model performance with dust heterogeneous chemistry. The TAQMN provides observations of most criteria air pollutants yet only PM₁₀ observations at the Xinzhuang site are used in this study to focus on dust storm impact. These variables are used to examine the simulation responses by implementing dust heterogeneous chemistry. Ground-based measurements of K⁺, Mg₂⁺, Ca₂⁺, and PM_{2.5} at Duolun and Yunlin from Fudan University's observation network (Huang et al., 2010) are used to investigate the model's capability of simulating tracer metals by applying the source-dependent speciation profile for suspended dust particles. AOD from the AERosol RObotic NETwork (AERONET; <http://aeronet.gsfc.nasa.gov/>) operated by NASA is also collected to evaluate the CMAQ predictions. To examine the spatial distribution and column density of model-simulated dust particles, we also used AOD products from the Moderate Resolution Imaging Spectroradiometer (MODIS; <http://modis.gsfc.nasa.gov/>). [All observations are collected](#)

for the period of March and April from 2006 to 2010, except for the Fudan Univ. data which only covers March and April in 2007. The locations of observational stations by the API, EANET, TAQMN, and AERONET are indicated in Figure 2, along with the locations of Duolun and Yunlin. Table 4-5 summarizes the detailed information of each observation network.

3. Results

3.1 Improved model performance with revised friction velocity thresholds

To examine model improvement by implementing new initial threshold friction velocity constants, simulation results from Dust_Default and Dust_Revised are compared for the spatial distribution of PM₁₀ and evaluation bias against API. Dust_Default - Dust_Off, and Dust_Revised - Dust_Off represents the PM₁₀ from the default dust scheme and the revised dust scheme, respectively, as shown in Figures 3 (a) and (b). PM₁₀ concentrations generated from dust are averaged for March and April from 2006 to 2010. Figure 3 (a) indicates that the default dust scheme produces a very limited amount of PM₁₀ only over the Gobi Desert for less than 70µg/m³, which can hardly represent the East Asian dust storms. The revised scheme produces higher PM₁₀ concentrations as more than 400µg/m³ at the Gobi source region, as shown in Figure 3(b). Dust plumes are generated by the revised model over the Gobi and Taklamakan deserts, and also from sparse grassland over the northwest region of the Tibetan Plateau. Particles from dust plumes are transported southeastwardly and contributed 50~100µg/m³ of PM₁₀ over northern and eastern China, and less than 50µg/m³ over southern China, South Korea, and Japan. Huang et al. (2010) demonstrated that there are two transport pathways for Asian dust: plumes from the Gobi and Taklamakan are either pushed by prevailing winds eastward towards South Korea and Japan or southeastward down towards southern China and Taiwan. With the revised dust scheme, the CMAQ generally reproduces the spatial distribution of Asian dust as shown in Figure 3(b), which indicates the most significant impact over northern and eastern China and relatively weak impacts over downwind areas along the transport pathway towards southeast. Figures 3 (c) and (d) demonstrate the evaluation bias at the API cities over China for the Dust_Default and Dust_Revised

scenarios, respectively. With the default dust scheme, the CMAQ shows a large negative bias for the entire domain. Most serious underestimation is found over northern and western China, with a negative bias more than $-80\mu\text{g}/\text{m}^3$. Figure 3(c) also suggests that cities closer to the Taklamakan and Gobi deserts have larger negative bias, indicating that the default scheme cannot generate sufficient dust emission to reproduce the observed PM_{10} . With the revised scheme as shown in Figure 3 (d), simulation biases for most of the cities are reduced down to $\pm 20\mu\text{g}/\text{m}^3$. The largest overestimation is found at Hohhot as $39\mu\text{g}/\text{m}^3$, ~~with relatively larger discrepancy in cities close to the Gobi Desert. The and~~ the largest underestimation is found at Xining and Lanzhou ($-60\mu\text{g}/\text{m}^3$). ~~Figure 3(d) also indicates that model tend to have larger simulation discrepancy in cities close to the desert. These two cities are mainly affected by dust from the Taklamakan Desert, so dust emission from the Taklamakan might still be underestimated in the revised dust scheme.~~

Figures 4 (a) to (c) summarizes the evaluation statistics for simulated PM_{10} against observations from the API. Daily data pairs from observation and simulation are used here to calculate the statistics. The Dust_Off scenario underestimates PM_{10} concentration by -56.74%. Since dust storms from the Taklamakan and Gobi substantially contribute to suspended particle concentrations over East Asia during spring, simulation ~~without~~ with no dust emission should be responsible for the large underestimation. With the default dust emission module, model performance for the scenario Dust_Default is only slightly improved and PM_{10} is still underestimated by -55.42%, as shown by Figure 4(b). The comparison between Dust_Off and Dust_Default suggests that the default dust module is not able to generate sufficient elevated particles to match the observed PM_{10} levels from the API. On the other hand, the Dust_Revised scenario shows a much better performance with a NMB value of -16.06% as shown in Figure 4(c). Simulation results are also evaluated against AOD observations from the AERONET, with the statistics shown in Figures 4 (d) to (f). Statistics for AOD evaluation against the AERONET suggest similar model performances as for PM_{10} . The CMAQ simulation without dust rise underestimates AOD by -31.34% at AERONET stations, and the default dust module has almost no improvement for AOD prediction. The Dust_Revised scenario underestimates AOD by

-22.1%, indicating that the revised scheme is also able to improve the model performance for simulating fine mode dust.

3.2 Impacts of applying source-dependent profile

Speciation of dust particles determines the contributions of crust species and trace metal concentrations predicted by the model. As described in Section 2.2, we modified the fixed speciation profile within the CMAQ to be source-dependent for the Gobi and Taklamakan, respectively, and in this section ground-based observations collected at Duolun and Yulin are used to investigate the impacts by applying different speciation profiles. The model simulations from the Dust_Revised and Dust_Profile scenarios are compared with observations for K^+ , Mg_2^+ , and Ca_2^+ with data pairs, as shown in Figure 5 (simulations and observations for K^+ and Mg_2^+ are upscaled by 5 and 10 times, respectively, to make them comparable with Ca_2^+ in the same figure), and evaluation statistics are summarized in Table 56. The two cities are close to the Gobi Desert, as shown by Figure 2. Huang et al. (2010) used back trajectory and Ca/Al ratio analysis to demonstrate that the Gobi Desert is the main contributor for dust particles at Duolun and Yulin. Figure 5(a) indicates that with the default speciation profile, the CMAQ overestimates K^+ and Ca_2^+ by 208.9% and 36.69%, respectively. Predicted Mg_2^+ concentration is almost zero because there is no emission of Mg_2^+ in the anthropogenic emission inventories, and the default profile indicated zero percentage mass contribution of Mg_2^+ from dust emission. With the source-dependent speciation profile, the CMAQ simulation of Mg_2^+ is increased significantly as shown in Figure 5(b). The revised CMAQ underestimates K^+ and Ca_2^+ by -47.83% and -53.12%, respectively. Consistent negative bias for trace metals should due to the underestimation of total fine mode aerosol within dust. Figure 5(c) shows the comparison between observed and simulated $PM_{2.5}$ concentrations at Duolun and Yulin. The Dust_Revised and Dust_Profile scenarios only differ in terms of their speciation profile for particles. The predicted $PM_{2.5}$ from the two scenarios are almost identical, so only ~~one set of data pairs are~~ Dust_Profile is shown in Figure 5(c). ~~On the one hand, c~~Concentration of $PM_{2.5}$ is underestimated by -45.59%, which is consistent with the underestimations of Mg_2^+ , K^+ , and Ca_2^+ . The evaluation statistics suggest that total $PM_{2.5}$ is underestimated at Duolun and Yunlin, but Ca_2^+ is

overestimated under the default profile. So although the NMB value changes from 36.69% by default profile to -53.12% for Ca_2^+ by revised profile, it is highly possible that the revised profile provides a better estimation of the calcium mass contribution since the evaluation statics for trace metals should be consistent with that for total $PM_{2.5}$. The overall underestimation for $PM_{2.5}$ and trace metals should be due to the underestimation of fine mode aerosol mass contribution (20%) in total dust emission. On the other hand, simulation bias shown in Figure 3(d) suggests a slight overestimation of PM_{10} at cities close to the Gobi Desert. So it is highly possible that fine particle mass contribution configured within the CMAQ might be underestimated. Unfortunately, measurements made by Huang et al. (2010) only collected data for total suspended particles (TSP) and no PM_{10} observation is found for Duolun or Yulin. So no solid conclusion is made at this point because the PM_{10} data is not available at Duolun or Yulin, although the total suspended particles (TSP) is measured and indicate the fine mode aerosol should have larger mass contribution (about 40% in TSP). ~~The comparison between the Dust_Revised and Dust_Profile scenario suggests that the source-dependent speciation profile is more reasonable for predicting trace metals from dust emission.~~

3.3 Impacts of heterogeneous chemistry

Dust heterogeneous chemistry involves uptake of gas-phase species and production of secondary inorganic aerosols. In this section we investigate the impacts of implementing dust chemistry into the CMAQ by examining the simulation difference between Dust_Chem and Dust_Profile, and the difference between Dust_ChemHigh and Dust_Profile. Figure 6 shows the concentration changes (color contours represent the absolute concentration changes, and dash lines represent the percentage changes) under heterogeneous chemistry with lower (left column) and upper (right column) limits of uptake coefficients for O_3 (1st row), SO_2 (2nd row), SO_4^{2-} (3rd row), HNO_3 (4th row), NO_x (5th row), and NO_3^- (6th row). All variables are averaged for March and April from 2006 to 2010. The spatial distributions shown in Figure 6 suggest that impacts of dust chemistry are more pronounced in eastern China over the downwind areas than in the dust source area near the deserts. This is because eastern China has intense anthropogenic emissions that help to accelerate the dust chemistry, while the desert areas in northern and

western China have much lower concentrations of the reactive gases. Dong and Fu (2015a) reported that in spring, O₃ concentration is around 30ppbv and less than 5ppbv for NO₂ and SO₂ over the Gobi, while the concentrations over eastern China are 50~60ppbv for O₃ and 10~40ppbv for NO₂ and SO₂. More abundance of these reactive gases participate in the heterogeneous reactions on the surface of dust particles transported from deserts, and thus lead to a more significant impact of dust chemistry over the downwind area instead of over the deserts. Li et al. (2012) also reported that the impact of dust chemistry for O₃, SO₂, and NO₂ is less than 5% over the Gobi but up to 30~40% in eastern China and even higher over the western Pacific. O₃ concentration is reduced by 3~6 ppbv (2%~10%) and 5~11ppbv (4%~20%) with the lower and upper limits of uptake coefficients, respectively, due to irreversible reaction R1 as listed in Table 23, which agrees well with the values reported by Tang et al. (2004) as 20% and Li et al. (2012) as 5%~20%. Wang et al. (2012) reported lower O₃ reduction due to dust chemistry by 3.8ppbv and 7.3ppbv with lower and upper uptake coefficients, respectively, which could be because of using a different simulation year (2001) with a lower baseline O₃ over East Asia. Concentration of SO₂ is reduced by ~2 ppbv (10%) and ~6 ppbv (30%) with lower and upper limits of uptake coefficients, respectively, due to the consumption in reaction R13, which also leads to the increase of SO₄²⁻ concentration by ~3μg/m³ (8%) and more than 5μg/m³ (15%) under Dust_Chem and Dust_ChemHigh, respectively. Impacts on SO₂ reported by other studies have a moderate difference with a factor of 2 or more, varying from 55% by Tang et al. (2004) as the highest, 10%~20% as the medium (Li et al., 2012), and 5%~8% as the lowest (Wang et al., 2012). Different impacts caused by heterogeneous chemistry reported by different studies should mainly be attributed to the different simulation episodes. Tang et al. (2004) focused on dust episodes only in 2001 with lower baseline pollutants from anthropogenic emission, Li et al. (2012) also simulated dust episodes but in 2010, and Wang et al. (2012) simulated 2001 but focused on the entirety of April, where the monthly averages of particles are apparently smaller than values from dust episodes only. Reaction R7 indicates consumption and R11 indicates production of HNO₃, while the net effect of dust chemistry is found to decrease HNO₃ concentration by 0.2ppbv~0.8ppbv (8%~30%) as shown in Figures 6(e) and (f). Our result is comparable with the values reported by Li et al. (2012) as 5%~40%, but

1 smaller than that reported by Tang et al. (2004) as 30%~70%. Although the reaction R9
 2 indicates uptake of NO_x by dust particles, simulation results suggest that NO_x
 3 concentration is increased by 0.2ppbv~1ppbv over eastern China and the West Pacific.
 4 The elevation of NO_x concentration should be attributed to the [depletion of \$\text{O}_3\$ and the](#)
 5 conversion of gas-phase HNO_3 back to NO_x (Yarwood et al., 2005). As a result of
 6 excessive SO_4^{2-} production from dust chemistry, concentration of NO_3^- is decreased
 7 under the Dust_Chem scenario due to the thermal-dynamic equilibrium between SO_4^{2-} –
 8 $\text{NH}_4^+ - \text{NO}_3^-$. The equilibrium drives the inorganic aerosols to convert from NH_4NO_3 to
 9 $(\text{NH}_4)_2\text{SO}_4$ over eastern China with intensive anthropogenic SO_2 and NO_x emissions from
 10 industry and power sectors, but insufficient NH_3 to neutralize all the acid anions. On the
 11 other hand, over the western Pacific and Japan, where SO_2 and NO_x emissions are less
 12 intensive, concentration of NO_3^- is increased slightly due to the productions indicated by
 13 reactions R8 and R10. Consequently, over eastern and central China, removed NO_3^-
 14 evaporate back to HNO_3 , which again push the gas-phase equilibrium towards production
 15 of NO_x , and thus leads to the increase of NO_x but decrease of HNO_3 and NO_3^- .
 16 Meanwhile, with the upper limit of uptake coefficients, the production rate of HNO_3
 17 catches up with the removal rate of NO_3^- , which helps to slow down the decrease of
 18 NO_3^- over China and accelerate the increase of NO_3^- over the western Pacific and Japan.
 19 Our result is consistent with the findings from other studies. Wang et al. (2012) also
 20 reported the increase of NO_x and decrease of HNO_3 and NO_3^- concentrations due to dust
 21 chemistry over East Asia. Li et al. (2012) report that NO_3^- concentration with lower
 22 uptake coefficient is about $5\mu\text{g}/\text{m}^3$ (30%) lower than the base case simulation (with "best
 23 guess" uptake coefficient suggested in Zhu et al. (2010)), and NO_3^- predicted by high
 24 uptake coefficient is about $12\mu\text{g}/\text{m}^3$ (100%) higher than the base case at Shanghai and
 25 Xiamen.

26 The impact of dust chemistry shown in Figure 6 suggests comparable results as other
 27 modeling assessments, but very few previous studies incorporated observation data to
 28 validate further the impact indicated by the model. To evaluate the model's capability of
 29 representing dust chemistry and also determine the best fit uptake coefficients,
 30 observations from EANET are used to compare with simulations from Dust_Profile,
 31 Dust_Chem, and Dust_ChemHigh. Evaluation statistics are summarized in Table [67](#).

Simulation results from different scenarios for O_3 all agree well with observations as indicated by the statistics. O_3 is overpredicted by 1.26% without dust chemistry in the CMAQ, and underpredicted by -1.97% and -4.43% with lower and upper uptake coefficients, respectively. SO_2 is overpredicted in all scenarios, but the NMB value is reduced from 90.7% without dust chemistry to 69.8% and 63.7% with lower and upper uptake coefficients, respectively. Evaluation statistics for HNO_3 and NO_x show a similar response as SO_2 , where heterogeneous chemistry helps to reduce the large overestimations from 109.03% without dust chemistry to 85.17% and 81.24% with lower and upper limits of uptake coefficients, respectively. The positive bias for SO_2 and HNO_3 should be attributed to the overestimated anthropogenic emissions (Dong and Fu, 2015a; Wang et al., 2011). For NO_x evaluation, however, model overestimation is increased from 35.61% under the Dust_Profile scenario to 37.79% and 38.21% under the Dust_Chem and Dust_ChemHigh scenarios, respectively. Overestimation of NO_x emission should be responsible for the positive bias from the CMAQ as indicated by previous studies (Dong and Fu, 2015a), but implementing dust chemistry into the model leads to larger overprediction of NO_x . Concentration of SO_4^{2-} is underpredicted by 16.28% without dust chemistry, yet the simulation overpredicts SO_4^{2-} by 13.74% and 29.43% under Dust_Chem and Dust_ChemHigh scenarios, respectively. For NO_3^- predictions, dust chemistry helps to reduce the underprediction from 13.07% under the Dust_Profile scenario to -1.97% under Dust_Chem scenario. But the simulation is boosted up too much with upper limit of coefficients and it overpredicts NO_3^- concentration by 24.09% under the Dust_ChemHigh scenario. Note that EANET data are collected from Japanese sites so that Dust_Chem and Dust_ChemHigh show consistent increases of NO_3^- , as shown in Figure 6. Statistics shown in Table 6–7 suggest that implementing heterogeneous chemistry seems able to improve the CMAQ performance for most of the species except O_3 and NO_x , but the lower limit of uptake coefficients favors prediction of SO_4^{2-} and NO_3^- , and the upper limit of uptake coefficients has a better prediction for SO_4^{2-} and HNO_3 . Although these statistics show competitive performance between Dust_Chem and Dust_ChemHigh, the lower limit of the uptake coefficient might be more appropriate if we consider the uncertainty within the baseline anthropogenic emissions. With both surface observations and satellite retrievals, Dong and Fu (2015a)

demonstrated that the CMAQ overpredicted NO_x and SO_2 over East Asia between 2006 and 2010 by around 30% and 20%, respectively, due to overestimation in anthropogenic emissions. Wang et al. (2011) also report overestimation of SO_2 by 14% over China. Implementing dust chemistry helps to reduce simulated concentrations of SO_2 , NO_x , and HNO_3 , so it can balance part of the positive bias caused by anthropogenic emissions, but the statistics for SO_4^{2-} and NO_3^- indicate that the counter effect caused by using the upper limit of uptake coefficients might be too excessive and push the balance towards overestimation of aerosols as a side effect. Consequently, without explicitly excluding the bias within anthropogenic emissions, no solid conclusion could be achieved regarding the preference of uptake coefficients.

4. Discussion

4.1 Simulating a severe dust storm event

In this section we probe in to the capability of the CMAQ for reproducing a severe dust event. Many studies have reported that spring 2010 had the most severe dust storms in recent decades (Bian et al., 2011; Li et al., 2012) due to nation-wide drought in China. PM_{10} observations were more than $1,000\mu\text{g}/\text{m}^3$ at Beijing (Han et al., 2012), $1,600\mu\text{g}/\text{m}^3$ at Seoul (Tatarov et al., 2012), and $1,200\mu\text{g}/\text{m}^3$ at Taiwan (Tsai et al., 2013). These studies mainly focused on the impact of dust storms on a local scale, and the understanding about the emission and transport of the dust event on a regional scale is not well-developed. Here we examined this severe dust event with model simulations, satellite observations, and also surface measurements from multiple networks. Figure 7 displays the MODIS AOD and simulated AOD from the CMAQ Dust_Chem scenario during the severe dust storm episode from 19 to 21 March 2010. Simulated AOD is derived by following the approach described in Huang et al. (2013) for 11:00AM local time only to accommodate with the nadir view time by the MODIS. Spatial distributions of satellite agree well with the simulation on a daily scale, indicating that the model can generally reproduce the column density and long-range transport of dust particles. As shown in Figure 7 (b), the CMAQ simulation suggests that a large amount of dust emissions were uplifted on March 19th from the Gobi and increased AOD values over the

desert and northern China. The heavy dust emission on 19 March had been identified with OMI by Li et al. (2011), Figure 8 (a) also indicates consistently high AOD values around northern China. As the dust plume moved eastwards, both the MODIS and the CMAQ suggests that AOD in the eastern coastal area of China increased from about 0.8 on March 19th to more than 2.0 on March 20th. On March 21st, the majority of the dust plume was pushed eastward and started to build up AOD over the west Pacific and Japan.

To further examine the dust event, forward trajectory is analyzed to characterize the transport pathway of dust plumes with the Hybrid Single-Particle Lagrangian Integrated Trajectory (HYSPLIT) model from NOAA/Air Resources Laboratory (Draxler and Rolph, 2015; Rolph 2015). Movement of air mass was analyzed for 72 hours, starting from 0:00 UTC (8:00 local time) on March 19th, 2010 at the Gobi, with the forward trajectories shown in Figure 8(f). Air masses at 500 (red line), 1,000 (blue line), and 2,000 meters (green line) moved southeastward until March 20th, when the higher plume turned east and moved across Japan and the west Pacific, while the lower plumes continued towards the eastern coastal area of China and finally reached Taiwan on March 21st. The HYSPLIT trajectory showed consistent transport of dust plumes as the MODIS and the CMAQ AOD analysis.

To understand the impact of dust storms along the transport pathway, we compare the simulated and observed surface level PM₁₀ on a daily scale for all of March 2010 at selected stations along the transport pathway, as indicated by Figure 8(f). Simulations from the Dust_Chem (black lines in Figs. 8(a)-(e) and (g)-(o)) and the Dust_Off scenarios (blue lines in Fig. 8(a)-(e) and (g)-(o)) are analyzed to examine the model performance. Temporal variations of PM₁₀ with observations from the API (red circles) are examined at Beijing, Lanzhou, Nanjing, Fuzhou, Lianyungang, and Shanghai as shown in Figures 8(a), (b), (c), (d), (e), and (k), respectively. Observed PM₁₀ concentrations increased rapidly from less than 300µg/m³ on 18 March to more than 600µg/m³ at Beijing and 480µg/m³ at Lianyungang on 19 March. In central and eastern China, concentrations of PM₁₀ peaked on 21 March at Nanjing and Shanghai, and the API reached the measurement ceiling value of 600µg/m³. In southern China, PM₁₀ was also elevated to 600µg/m³ at Xiamen on 22 March. Temporal variation in these cities suggested that PM₁₀ concentrations were elevated with the onset of the dust storm, which moved from the Gobi to southeastern

1 China from 19 to 21 March. PM_{10} concentrations fell back under $300\mu\text{g}/\text{m}^3$ after the
2 event. Lanzhou reached a peak of PM_{10} concentration as $500\mu\text{g}/\text{m}^3$ on 14 March, which
3 should be attributed to the impact of the dust storm that originated from the Taklamakan.
4 Ling et al. (2011) also reported an observed $507\mu\text{g}/\text{m}^3$ PM_{10} on 14 March at Lanzhou.
5 Observations from EANET and the TAQMN are also employed to examine the
6 long-range transport of dust over the West Pacific and Taiwan. Temporal variations of
7 PM_{10} at three EANET sites (green diamonds) including Oki, Ogasawara, and Hedo are
8 shown in Figures 8(h), (i), and (j), respectively. PM_{10} concentrations at these sites all
9 showed consistent increase with the onset of dust on 21 or 22 March. At Xinzhuang, as
10 shown in Figure 8(g), observations from the TAQMN (purple circles) demonstrated that
11 local PM_{10} was increased from less than $100\mu\text{g}/\text{m}^3$ on 20 March to more than $700\mu\text{g}/\text{m}^3$
12 on 21 March due to the impact of the dust storm. Simulated PM_{10} from the Dust_Chem
13 scenario agreed well with observations from different networks all over the domain.
14 Predictions from the Dust_Chem and Dust_Off scenarios were almost the same at all
15 stations during the non-dust period from 1 to 10 March, yet the Dust_Chem scenario was
16 able to reproduce the rapid elevation of PM_{10} during the dust event. However, noticeable
17 discrepancy was also found between the Dust_Chem prediction and observations. In
18 general, the CMAQ overpredicted PM_{10} slightly during the dust event at most of the API
19 sites in China, but failed to reproduce the high concentrations at Lanzhou before 15
20 March and after 20 March. To help understand the model performance of predicting fine
21 particles from dust, daily variations of AOD from the AERONET observations and the
22 CMAQ simulations are also examined at four stations, including Beijing, the Semi-Arid
23 Climate Observatory Laboratory (SACOL) station at Lanzhou (Ling et al., 2011), Osaka,
24 and EPA-NCU (Taiwan Environment Protection Agency station at National Central
25 University), as show in Figures 9 (l), (m), (n), and (o), respectively. Temporal variations
26 of AOD were consistent with the daily changes of PM_{10} at these cities along the dust
27 plume movement trajectory. The highest AOD was found on 14 March at the SACOL
28 station, which was consistent with the rapid increase of PM_{10} concentrations at Lanzhou.
29 Moderate underestimations of AOD were also found at Lanzhou and EPA-NCU stations
30 during the dust events, indicating that fine mode aerosols were also underestimated over
31 this region. In general, comparisons between the CMAQ and observations from MODIS

and surface networks suggest that the model is capable of reproducing the severe dust storm event in terms of spatial distribution, transport, and concentration of dust particles, with possible underestimation of dust emission from the Taklamakan.

4.2 Remaining uncertainties within the modeling system

Despite the improvements of model performance demonstrated in the previous sections, it is necessary to note that there are some important remaining uncertainties within the modeling system. The first type of uncertainty is related to the anthropogenic emissions. Assessment of dust prediction capability of the model was primarily performed by comparing the simulation with observations, yet the bias caused by anthropogenic emissions would affect the bias from the dust prediction. So it is difficult to distinguish the uncertainties that arise from dust treatment in the model. Figure 9 displays the dust emission rate (Tg/day) from the Dust_Chem scenario (blue rectangles, with blue dash line indicating the trend), simulation bias of PM₁₀ at the API stations (red circles, with red dash line indicating the trend), and simulation bias of PM₁₀ at EANET stations (green diamonds, with green dash line indicating the trend), with all variables averaged on monthly scale. Prediction from the CMAQ suggests a slightly increasing trend of dust emission from 2006 to 2010, which is consistent with the decadal increase of dust reported by Kurosaki et al. (2011) due to changes of soil erodibility over Mongolia and northeastern China. The recent decadal trend of dust emission over East Asia remains an open-ended question that will rely on investigate with longer term simulations. Simulation biases of PM₁₀ agree fairly well with the dust emission at both the API and EANET stations, indicating that overall underprediction of PM₁₀ over East Asia has a smaller discrepancy for years with stronger dust events. Assuming there is persistent underestimation of primary PM emissions in the anthropogenic inventory, more dust emissions will apparently help to reduce the modeling bias for total PM₁₀. This is also consistent with previous studies (Wang et al., 2011; Dong and Fu. 2015a) which reported a systematic underestimation of anthropogenic emission of primary particles over China.

The second type of uncertainty lies within the friction velocity threshold u_{*t} , which is affected by soil moisture fraction that might be overestimated by the WRF. Although in this study the simulation performance is improved with the initial threshold friction

velocity constants u_{*c} adjusted by avoiding the double counting of soil moisture effect,
 there are still non-negligible biases as shown in Section 3. Both the five-year average
 modeling bias shown in Figure 3(d) and temporal variations shown in Figure 8 suggest
 possible overestimated dust emission from the Gobi and underestimated dust from the
 Taklamakan. The averaged u_{*t} calculated by the CMAQ is 0.19m/s and 0.14m/s over
 the Taklamakan and Gobi, respectively, with the soil moisture factor f_{soilm} as 1.21 and
 1.13, respectively, indicating that the Taklamakan needs higher friction velocity in order
to generate dust. ~~As compared to the Gobi, the Taklamakan requires higher friction~~
~~velocity to generate dust~~ because of a more significant soil moisture impact. However,
 some recent field measurement studies suggest that the u_{*t} in the Taklamakan is lower
 than that over the Gobi. He et al. (2010) conducted measurements at three sites inside the
 Taklamakan and reported the value of u_{*t} as 0.25m/s, 0.27m/s, and 0.21m/s at three
 different sites, and Yang et al. (2011) also reported the value of u_{*t} as 0.24 m/s at
 Tazhong (~39.03°N, 83.65°E). For the Gobi, Li and Zhang (2011) reported the value of
 u_{*t} as 0.34 m/s ~0.42 m/s based on measurements made in April 2006 and 2008. Field
 measurements defined u_{*t} as equal to the value of friction velocity u_* when dust
 concentration is increased by 20% for at least one-half hour (Li and Zhang, 2011), thus
 the reported values of u_{*t} from the measurement studies are higher than the calculations
 from the model. But the comparison between the Taklamakan and Gobi measurements
 suggests that the model may either underestimate at the Gobi or overestimate at the
 Taklamakan for u_{*t} . Since f_{soilm} is determined by soil moisture fraction, we compare
 the soil moisture from FNL (NCEP final analysis data) which is used to drive WRF in
 this study with another reanalysis dataset GLDAS (Global Land Data Assimilation
 System; (Rodell et al., 2004)). Figure 10 demonstrates the five-year averages (for
 March and April) of soil moisture fraction at top 10cm depth from (a) FNL and (b)
 GLDAS. Soil moisture is estimated to be 10~15% by FNL at both deserts, while the
 values from GLDAS are less than 5% at the Taklamakan and 5%~10% at the Gobi.
 Zender et al. (2003) reported that soil moisture from NCEP is too high over active dust
 emission areas and leads to negative AOD bias of the model on a global scale. With the

1 WRF-NMMB/BSC-Dust model, Haustein et al. (2012) conducted simulations with
2 meteorology driven by FNL and GLDAS respectively over north Africa and reported that
3 the predictions with GLDAS had better agreement with the AERONET's AOD
4 observations due to smaller friction velocity and slightly faster surface wind speed due to
5 lower values of soil moisture. But no such sensitivity studies have been made over East
6 Asia, and unfortunately there is no publicly available observation data for the period of
7 2006-2010 to examine the potential overestimation of soil moisture by FNL in our
8 modeling domain. Although we previously reported consistent negative bias of surface
9 temperature at 2 meters height for 2006-2010, which might be due to excessive soil
10 moisture (Dong and Fu, 2015), more research efforts are required to verify the
11 uncertainties caused by using FNL soil data.

12
13 The last type of uncertainty lies within the mass contribution of fine aerosols within dust
14 emission. Elevated dust particles are distributed into fine and coarse mode aerosols with
15 mass ratios of 0.2 and 0.8, respectively, in the CMAQ dust scheme. In this study however,
16 the ratio of $PM_{2.5}$ /TSP derived from observations at Duolun and Yulin are 0.42 and 0.39,
17 respectively, indicating that fine particles should have higher mass contribution within
18 East Asian dust. The data from Huang et al. (2010) indicated that the ratio of $PM_{2.5}$ /TSP
19 at Tazhong was 0.45 in spring 2007, which suggested an even higher fine particle mass
20 contribution at the Taklamakan. Model evaluation results shown in Figure 5 also
21 demonstrate the systematic underestimations of both trace metals and total $PM_{2.5}$
22 concentrations at both dust source regions and downwind areas, while the concentrations
23 of PM_{10} are slightly overestimated near the source region as demonstrated in Figure 3.
24 Consequently, it is highly possible that the ratio of fine particles within dust emission
25 should be higher. But since TSP also include all large particles $>10\mu m$, observations of
26 both $PM_{2.5}$ and PM_{10} at active dust regions are urgently needed to help clearly
27 characterize the ratio in the model.

5. Summary

~~Model development has been implemented into the CMAQ~~The dust module in CMAQ has been further developed in this study. The initial threshold friction velocity constants are revised by removing the double counting of soil moisture in the default parameters; two source-dependent speciation profiles are derived based on local observations of dust emission from the Taklamakan and Gobi deserts; and dust heterogeneous chemistry is implemented. The CMAQ with its revised dust scheme is applied over East Asia for March and April from 2006 to 2010. Based on model evaluations with observation data from both ground-surface networks and satellite retrievals, the revised dust scheme is demonstrated to improve the model performance. Evaluation statistics suggest that NMB for PM₁₀ simulation is reduced from -55% by default model to -16% by the revised model, and NMB for AOD is reduced from -31% to -22%. Applying source-dependent speciation profiles improves the simulation of trace metals. Heterogeneous chemistry with lower and upper limits of uptake coefficients is also investigated. Although simulations with dust chemistry are demonstrated to agree with observations better than those without chemistry for most of the pollutants, no solid conclusion could be made regarding the preference of uptake coefficients without explicitly excluding the uncertainty caused by anthropogenic emission. This is because simulation with lower coefficients has better agreement with observations for O₃, SO₄²⁻, and NO₃⁻, while simulation with upper coefficients has better performance for SO₂ and NO₂.

A severe dust storm episode from 19 to 21 March 2010 is investigated to examine the model performance during extreme dust event. The revised CMAQ modeling system successfully reproduces most of the PM₁₀ and AOD observations in both near source (China) and downwind areas (Japan and Taiwan). But some notable discrepancies are also found, indicating the slight overestimation of dust from the Gobi and underestimation of dust from the Taklamakan. Comparison of the FNL and GLDAS soil moisture fractions indicates that the excessive soil moisture within FNL might be responsible for the higher friction velocity threshold and lower dust emissions calculated by the CMAQ over the Taklamakan. But more sensitive studies with different reanalysis data inputs for WRF and the local soil moisture measurements in the deserts are needed to reach a solid conclusion. In addition, potential uncertainty is also identified within the

1 mass contributions of fine and coarse mode particles from dust emission. Evaluation
2 results indicate consistent underestimation of trace metals and $PM_{2.5}$ by 30%~50% at
3 Duolun and Yulin close to the Gobi desert, yet the PM_{10} are generally overestimated
4 slightly at adjacent cities. While measurements from Huang et al. (2010) suggested mass
5 contribution as ~40% of fine particles in TSP, the value of 20% used in the current
6 CMAQ might be too low for dust emissions from the Gobi and Taklamakan. In summary,
7 the model development employed in this study has been demonstrated to enhance the
8 capability of the CMAQ for simulating dust over East Asia regarding the chemical and
9 physical processes involved, which can serve as a useful tool for further investigating the
10 impacts of dust on regional climate over East Asia and elsewhere.

11 12 **6. Acknowledgements**

13 We thank NASA GSFC (Grant No. NNX09AG75G) and the National Natural Science
14 Foundation of China (Grant No. 41429501) for their funding support. D. Tong is also
15 particularly grateful for his award of a NASA ROSES grant (NNX13AO45G). We would
16 like to acknowledge Edward J. Hyer for providing biomass burning emission, and we
17 thank Dr. Keiichi Sato and Dr. Ayako Aoyagi from the Asia Center for Air Pollution
18 Research for providing the EANET data. We would like to acknowledge Dr. George Lin
19 of the National Center University for providing the AOD observations from Taiwan, and
20 we would also like to acknowledge China MEP and Taiwan EPA for providing the
21 observation data, and thank NASA for providing the AERONET and MODIS data. We
22 thank the National Institute for Computational Sciences (NICS) for providing the
23 computer sources for the model simulations used in this research.

References

- Appel, K. W., Pouliot, G. A., Simon, H., Sarwar, G., Pye, H. O. T., Napelenok, S. L., Akhtar, F., and Roselle, S. J.: Evaluation of dust and trace metal estimates from the Community Multiscale Air Quality (CMAQ) model version 5.0, Geoscientific Model Development, 6, 883-899, 2013.
- Arimoto, R., Kim, Y. J., Kim, Y. P., Quinn, P. K., Bates, T. S., Anderson, T. L., Gong, S., Uno, I., Chin, M., Huebert, B. J., Clarke, A. D., Shinozuka, Y., Weber, R. J., Anderson, J. R., Guazzotti, S. A., Sullivan, R. C., Sodeman, D. A., Prather, K. A., and Sokolik, I. N.: Characterization of Asian Dust during ACE-Asia, Global and Planetary Change, 52, 23-56, 2006.
- Bauer, S. E., Balkanski, Y., Schulz, M., Hauglustaine, D. A., and Dentener, F.: Global modeling of heterogeneous chemistry on mineral aerosol surfaces: Influence on tropospheric ozone chemistry and comparison to observations, Journal of Geophysical Research-Atmospheres, 109, D02304, DOI: 10.1029/2003JD003868 2004.
- Bian, H., Tie, X. X., Cao, J. J., Ying, Z. M., Han, S. Q., and Xue, Y.: Analysis of a Severe Dust Storm Event over China: Application of the WRF-Dust Model, Aerosol and Air Quality Research, 11, 419-428, 2011.
- Bian, H. S., and Zender, C. S.: Mineral dust and global tropospheric chemistry: Relative roles of photolysis and heterogeneous uptake, Journal of Geophysical Research-Atmospheres, 108, 4672, doi:10.1029/2002JD003143, 2003.
- Blanco, A., De Tomasi, F., Filippo, E., Manno, D., Perrone, M. R., Serra, A., Tafuro, A. M., and Tepore, A.: Characterization of African dust over southern Italy, Atmospheric Chemistry and Physics, 3, 2147-2159, 2003.
- Carmichael, G. R., Tang, Y., Kurata, G., Uno, I., Streets, D., Woo, J. H., Huang, H., Yienger, J., Lefer, B., Shetter, R., Blake, D., Atlas, E., Fried, A., Apel, E., Eisele, F., Cantrell, C., Avery, M., Barrick, J., Sachse, G., Brune, W., Sandholm, S., Kondo, Y., Singh, H., Talbot, R., Bandy, A., Thornton, D., Clarke, A., and Heikes, B.: Regional-scale chemical transport modeling in support of the analysis of observations obtained during the TRACE-P experiment, Journal of Geophysical Research-Atmospheres, 108, 8823, doi:10.1029/2002JD003117, 2003.
- Chen, S. Y., Huang, J. P., Zhao, C., Qian, Y., Leung, L. R., and Yang, B.: Modeling the transport and radiative forcing of Taklimakan dust over the Tibetan Plateau: A case study in the summer of 2006, Journal of Geophysical Research-Atmospheres, 118, 797-812, 2013.
- Chun, Y. S., Boo, K. O., Kim, J., Park, S. U., and Lee, M.: Synopsis, transport, and physical characteristics of Asian dust in Korea, Journal of Geophysical Research-Atmospheres, 106, 18461-18469, 2001.
- Cwiertny, D. M., Young, M. A., and Grassian, V. H.: Chemistry and photochemistry of mineral dust aerosol, Annual Review of Physical Chemistry, 59, 27-51, 2008.
- Darmenova, K. and Sokolik, I.N.: Dust emission and deposition in regional models, Third International Dust Workshop, Leipzig, Germany, September, (September 15, 01-03) 2008
- Davis, J. M., Bhawe, P. V., and Foley, K. M.: Parameterization of N₂O₅ reaction probabilities on the surface of particles containing ammonium, sulfate, and nitrate, Atmospheric Chemistry and Physics, 8, 5295-5311, 2008.
- De Longueville, F., Hountondji, Y. C., Henry, S., and Ozer, P.: What do we know about effects of desert dust on air quality and human health in West Africa compared to other regions? Science of the Total Environment, 409, 1-8, 2010.

1 Dentener, F. J., Carmichael, G. R., Zhang, Y., Lelieveld, J., and Crutzen, P. J.: Role of mineral aerosol as a
2 reactive surface in the global troposphere, *Journal of Geophysical Research-Atmospheres*, 101,
3 22869-22889, 1996.

4 Dong, X. Y., Li, J., Fu, J. S., Gao, Y., Huang, K., and Zhuang, G. S.: Inorganic aerosols responses to
5 emission changes in Yangtze River Delta, China, *Science of the Total Environment*, 481, 522-532, 2014.

6 Dong, X. Y., and Fu, J. S.: Understanding interannual variations of biomass burning from Peninsular
7 Southeast Asia, part I: Model evaluation and analysis of systematic bias, *Atmospheric Environment*, 116,
8 293-307, 2015a.

9 Dong, X. Y., and Fu, J. S.: Understanding interannual variations of biomass burning from Peninsular
10 Southeast Asia, part II: Variability and different influences in lower and higher atmosphere levels,
11 *Atmospheric Environment*, 115, 9-18, 2015b.

12 Draxler, R.R. and Rolph, G.D.: HYSPLIT (HYbrid Single-Particle Lagrangian Integrated Trajectory)
13 Model access via NOAA ARL READY Website (<http://ready.arl.noaa.gov/HYSPLIT.php>). August 1st,
14 2015, NOAA Air Resources Laboratory, Silver Spring, MD, 2015

15 EANET: EANET Data Report 2006, Acid Deposition Monitoring Network in East Asia (EANET), 2007.

16 Engelstaedter, S., Kohfeld, K. E., Tegen, I., and Harrison, S. P.: Controls of dust emissions by vegetation
17 and topographic depressions: An evaluation using dust storm frequency data, *Geophysical Research Letters*,
18 30, 1294, doi:10.1029/2002GL016471, 2003.

19 Fairlie, T. D., Jacob, D. J., Dibb, J. E., Alexander, B., Avery, M. A., van Donkelaar, A., and Zhang, L.:
20 Impact of mineral dust on nitrate, sulfate, and ozone in transpacific Asian pollution plumes, *Atmospheric*
21 *Chemistry and Physics*, 10, 3999-4012, 2010.

22 F'ecan, F., Marticorena, B., and Bergametti, G.: Parametrization of the increase of the aeolian erosion
23 threshold wind friction velocity due to soil moisture for arid and semi-arid areas, *Ann. Geophys.*, 17, 149–
24 157, 1999.

25 Formenti, P., Elbert, W., Maenhaut, W., Haywood, J., and Andreae, M. O.: Chemical composition of
26 mineral dust aerosol during the Saharan Dust Experiment (SHADE) airborne campaign in the Cape Verde
27 region, September 2000, *Journal of Geophysical Research-Atmospheres*, 108, 8576,
28 doi:10.1029/2002JD002648, 2003.

29 Forster, P., Ramaswamy, V., Artaxo, P., Berntsen, T., Betts, R., Fahey, D. W., Haywood, J., Lean, J., Lowe,
30 D. C., Myhre, G., Nganga, J., Prinn, R., Raga, G., Schulz, M., and Van Dorland, R.: Radiative Forcing of
31 Climate Change, in *Climate Change 2007: The Physical Science Basis. Contribution of Working Group I to*
32 *the Fourth Assessment Report of the Intergovernmental Panel on Climate Change*, edited by S. Solomon, D.
33 Qin, M. Manning, Z. Chen, M. Marquis, K. B. Averyt, M. Tignor, and H. L. Miller, pp. 129–234,
34 Cambridge Univ. Press, Cambridge, United Kingdom and New York, NY, USA, 2007.

35 Fu, X., Wang, S.X., Cheng, Z., Xing, J., Zhao, B., Wang, J.D., and Hao, J.M.: Source, transport and
36 impacts of a heavy dust event in the Yangtze River Delta, China, in 2011. *Atmospheric Chemistry and*
37 *Physics*, 14(3) 1239-1254, 2014

38 Gillette, D.A., Adams, J., Endo, A., Smith, D., and Kihl, R.: Threshold Velocities for Input of Soil Particles
39 into the Air by Desert Soils. *Journal of Geophysical Research-Oceans and Atmospheres*, 85(Nc10)
40 5621-5630, 1980.

1 Gillette, D. A., Adams, J., Muhs, D., and Kihl, R.: Threshold friction velocities and rupture moduli for
2 crusted desert soils for the input of soil particles into the air, *Journal of Geophysical*
3 *Research*, 87, 9003– 9015, 1982.

4 Ginoux, P., Chin, M., Tegen, I., Prospero, J. M., Holben, B., Dubovik, O., and Lin, S. J.: Sources and
5 distributions of dust aerosols simulated with the GOCART model, *Journal of Geophysical*
6 *Research-Atmospheres*, 106, 20255-20273, 2001.

7 Grell, G. A., Peckham, S. E., Schmitz, R., McKeen, S. A., Frost, G., Skamarock, W. C., and Eder, B.: Fully
8 coupled "online" chemistry within the WRF model, *Atmospheric Environment*, 39, 6957-6975, 2005.

9 Guenther, A., Karl, T., Harley, P., Wiedinmyer, C., Palmer, P. I., and Geron, C.: Estimates of global
10 terrestrial isoprene emissions using MEGAN (Model of Emissions of Gases and Aerosols from Nature),
11 *Atmospheric Chemistry and Physics*, 6, 3181-3210, 2006.

12 Han, X., Ge, C., Tao, J. H., Zhang, M. G., and Zhang, R. J.: Air Quality Modeling for a Strong Dust Event
13 in East Asia in March 2010, *Aerosol and Air Quality Research*, 12, 615-628, 2012.

14 Haustein, K., Perez, C., Baldasano, J. M., Jorba, O., Basart, S., Miller, R. L., Janjic, Z., Black, T., Nickovic,
15 S., Todd, M. C., Washington, R., Muller, D., Tesche, M., Weinzierl, B., Esselborn, M., and Schladitz, A.:
16 Atmospheric dust modeling from meso to global scales with the online NMMB/BSC-Dust model - Part 2:
17 Experimental campaigns in Northern Africa, *Atmospheric Chemistry and Physics*, 12, 2933-2958, 2012.

18 Heikes, B. G., and Thompson, A. M.: Effects of Heterogeneous Processes on NO_3 , HONO, and HNO_3
19 Chemistry in the Troposphere, *Journal of Geophysical Research-Oceans and Atmospheres*, 88, 883-895,
20 1983.

21 Huang, K., Zhuang, G. S., Li, J. A., Wang, Q. Z., Sun, Y. L., Lin, Y. F., and Fu, J. S.: Mixing of Asian dust
22 with pollution aerosol and the transformation of aerosol components during the dust storm over China in
23 spring 2007, *Journal of Geophysical Research-Atmospheres*, 115, D00K13, doi:10.1029/2009JD013145,
24 2010.

25 Huang, K., Fu, J. S., Hsu, N. C., Gao, Y., Dong, X., Tsay, S.-C., and Lam, Y. F.: Impact assessment of
26 biomass burning on air quality in Southeast and East Asia during BASE-ASIA, *Atmospheric Environment*,
27 78, 291–302, doi:10.1016/j.atmosenv.2012.03.048, 2013.

28 Huneus, N., et al.: Global dust model intercomparison in AeroCom phase I, *Atmospheric Chemistry and*
29 *Physics*, 11(15), 7781–7816, 2011.

30 Kandler, K., Benker, N., Bundke, U., Cuevas, E., Ebert, M., Knippertz, P., Rodriguez, S., Schutz, L., and
31 Weinbruch, S.: Chemical composition and complex refractive index of Saharan Mineral Dust at Izana,
32 Tenerife (Spain) derived by electron microscopy, *Atmospheric Environment*, 41, 8058-8074, 2007.

33 Krueger, B. J., Grassian, V. H., Cowin, J. P., and Laskin, A.: Heterogeneous chemistry of individual
34 mineral dust particles from different dust source regions: The importance of particle mineralogy,
35 *Atmospheric Environment*, 38, 6253-6261, 2004.

36 Kumar, R., Barth, M. C., Pfister, G. G., Naja, M., and Brasseur, G. P.: WRF-Chem simulations of a typical
37 pre-monsoon dust storm in northern India: Influences on aerosol optical properties and radiation budget,
38 *Atmospheric Chemistry and Physics*, 14, 2431-2446, 2014.

39 Kurosaki, Y., and Mikami, M.: Regional difference in the characteristic of dust event in East Asia:
40 Relationship among dust outbreak, surface wind, and land surface condition, *Journal of the Meteorological*
41 *Society of Japan*, 83A, 1-18, 2005.

- 1 Lam, Y. F., and Fu, J. S.: A novel downscaling technique for the linkage of global and regional air quality
2 modeling, *Atmospheric Chemistry and Physics*, 9, 9169-9185, 2009.
- 3 Li, J., Wang, Z. F., Zhuang, G., Luo, G., Sun, Y., and Wang, Q.: Mixing of Asian mineral dust with
4 anthropogenic pollutants over East Asia: A model case study of a super-duststorm in March 2010,
5 *Atmospheric Chemistry and Physics*, 12, 7591-7607, 2012.
- 6 Li, J. W., Han, Z. W., and Zhang, R. J.: Model study of atmospheric particulates during dust storm period
7 in March 2010 over East Asia, *Atmospheric Environment*, 45, 3954-3964,
8 doi:10.1016/j.atmosenv.2011.04.068, 2011.
- 9 Li, W. Y., Shen, Z. B., Lu, S. H., and Li, Y. H: Sensitivity Tests of Factors Influencing Wind Erosion,
10 *Journal of Desert Research*, 27, 984-993, 2007.
- 11 Li, X. and Zhang, H. S.: Research on threshold friction velocities during dust events over the Gobi Desert
12 in northwest China, *Journal of Geophysical Research*, 116, D20210, doi:10.1029/2010JD015572, 2011.
- 13 Liao, H., Seinfeld, J. H., Adams, P. J., and Mickley, L. J.: Global radiative forcing of coupled tropospheric
14 ozone and aerosols in a unified general circulation model, *Journal of Geophysical Research-Atmospheres*,
15 109, D16207, doi:10.1029/2003JD004456, 2004.
- 16 Ling, X., Guo, W., Zhao, Q., and Zhang, B.: A case study of a typical dust storm event over the Loess
17 Plateau of northwest China *Atmos. Ocean. Sci. Lett.*, 4 (6), 344-348, 2011.
- 18 Liu, M., and Westphal, D. L.: A study of the sensitivity of simulated mineral dust production to model
19 resolution, *Journal of Geophysical Research-Atmospheres*, 106, 18099-18112, 2001.
- 20 Ma, C. J., Kasahara, M., Holler, R., and Kamiya, T.: Characteristics of single particles sampled in Japan
21 during the Asian dust-storm period, *Atmospheric Environment*, 35, 2707-2714, 2001.
- 22 Marticorena, B., Bergametti, G., Aumont, B., Callot, Y., NDoume, C., and Legrand, M.: Modeling the
23 atmospheric dust cycle .2. Simulation of Saharan dust sources. *Journal of Geophysical*
24 *Research-Atmospheres*, 102(D4) 4387-4404, 1997.
- 25 Matsuki, A., Iwasaka, Y., Shi, G. Y., Zhang, D. Z., Trochkin, D., Yamada, M., Kim, Y. S., Chen, B.,
26 Nagatani, T., Miyazawa, T., Nagatani, M., and Nakata, H.: Morphological and chemical modification of
27 mineral dust: Observational insight into the heterogeneous uptake of acidic gases, *Geophysical Research*
28 *Letters*, 32, L22806, doi:10.1029/2005GL024176, 2005.
- 29 Miller, R. L., Cakmur, R. V., Perlwitz, J., Geogdzhayev, I. V., Ginoux, P., Koch, D., Kohfeld, K. E.,
30 Prigent, C., Ruedy, R., Schmidt, G. A., and Tegen, I.: Mineral dust aerosols in the NASA goddard institute
31 for Space Sciences ModelE atmospheric general circulation model, *Journal of Geophysical*
32 *Research-Atmospheres*, 111, D06208, doi:10.1029/2005JD005796, 2006.
- 33 Muller, J. F., Stavrou, T., Wallens, S., De Smedt, I., Van Roozendaal, M., Potosnak, M. J., Rinne, J.,
34 Munger, B., Goldstein, A., and Guenther, A. B.: Global isoprene emissions estimated using MEGAN,
35 ECMWF analyses and a detailed canopy environment model, *Atmospheric Chemistry and Physics*, 8,
36 1329-1341, 2008.
- 37 Owen, P.R.: Saltation of uniform grains in air. *Journal of Fluid Mechanics*, 20(2), 225-242, 1964
- 38 Park, S. U., and In, H. J.: Parameterization of dust emission for the simulation of the yellow sand (Asian
39 dust) event observed in March 2002 in Korea, *Journal of Geophysical Research-Atmospheres*, 108, 4618,
40 doi:10.1029/2003JD003484, 2003.

- 1 Pathak, R. K., Wang, T., and Wu, W. S.: Nighttime enhancement of PM_{2.5} nitrate in ammonia-poor
2 atmospheric conditions in Beijing and Shanghai: Plausible contributions of heterogeneous hydrolysis of
3 N₂O₅ and HNO₃ partitioning, *Atmospheric Environment*, 45, 1183-1191, 2011.
- 4 Prospero, J. M.: Long-term measurements of the transport of African mineral dust to the southeastern
5 United States: Implications for regional air quality, *Journal of Geophysical Research-Atmospheres*, 104,
6 15917-15927, 1999.
- 7 Pun, B. K., and Seigneur, C.: Sensitivity of particulate matter nitrate formation to precursor emissions in
8 the California San Joaquin Valley, *Environmental Science & Technology*, 35, 2979-2987, 2001.
- 9 Qian, W. H., Quan, L. S., and Shi, S. Y.: Variations of the dust storm in China and its climatic control,
10 *Journal of Climate*, 15, 1216-1229, 2002.
- 11 Reddy, M. S., Boucher, O., Balkanski, Y., and Schulz, M.: Aerosol optical depths and direct radiative
12 perturbations by species and source type, *Geophysical Research Letters*, 32, L12803,
13 doi:10.1029/2004GL02174, 2005.
- 14 Reid, E. A., Reid, J. S., Meier, M. M., Dunlap, M. R., Cliff, S. S., Broumas, A., Perry, K., and Maring, H.:
15 Characterization of African dust transported to Puerto Rico by individual particle and size segregated bulk
16 analysis, *Journal of Geophysical Research-Atmospheres*, 108, 8591, doi:10.1029/2002JD00293, 2003.
- 17 Reid, J. S., Hyer, E. J., Prins, E. M., Westphal, D. L., Zhang, J. L., Wang, J., Christopher, S. A., Curtis, C.
18 A., Schmidt, C. C., Eleuterio, D. P., Richardson, K. A., and Hoffman, J. P.: Global Monitoring and
19 Forecasting of Biomass-Burning Smoke: Description of and Lessons From the Fire Locating and Modeling
20 of Burning Emissions (FLAMBE) Program, *IEEE Journal of Selected Topics in Applied Earth
21 Observations and Remote Sensing*, 2, 144-162, 2009.
- 22 Rogers, E., Springs, C., Black, G.T., Ferrier, M.B., Gayno, G., Janjic, Z., Lin, Y., Pyle, M., Wong, V., Wu,
23 W.S., and J.Carley: The NCEP North American Mesoscale modeling system: Recent changes and future
24 plans. Preprints, 23rd Conf. on Weather Analysis and Forecasting/19th Conf. on Numerical Weather
25 Prediction, Omaha, NE, Amer. Meteor. Soc., 2A.4, 2009 [Available online at [http://ams.confex.com/](http://ams.confex.com/ams/pdfpapers/154114.pdf)
26 [ams/pdfpapers/154114.pdf](http://ams.confex.com/ams/pdfpapers/154114.pdf)]
- 27 Rodell, M., Houser, P. R., Jambor, U., Gottschalck, J., Mitchell, K., Meng, C. J., Arsenault, K., Cosgrove,
28 B., Radakovich, J., Bosilovich, M., Entin, J. K., Walker, J. P., Lohmann, D., and Toll, D.: The global land
29 data assimilation system, *B Am Meteorol Soc*, 85, 381+, 10.1175/Bams-85-3-381, 2004.
- 30 Rosenfeld, D., Rudich, Y., and Lahav, R.: Desert dust suppressing precipitation: A possible desertification
31 feedback loop, *Proceedings of the National Academy of Sciences of the United States of America*, 98,
32 5975-5980, 2001.
- 33 Rolph, G.D.: Real-time Environmental Applications and Display sYstem (READY) Website
34 (<http://ready.arl.noaa.gov>), August 1st, 2015, NOAA Air Resources Laboratory, Silver Spring, MD, 2015
- 35 Sarwar, G., Roselle, S. J., Mathur, R., Appel, W., Dennis, R. L., and Vogel, B.: A comparison of CMAQ
36 HONO predictions with observations from the northeast oxidant and particle study, *Atmospheric*
37 *Environment*, 42, 5760-5770, 2008.
- 38 Shao, Y., and Dong, C. H.: A review on East Asian dust storm climate, modelling and monitoring, *Global*
39 *and Planetary Change*, 52, 1-22, 2006.
- 40 Simon, H., Beck, L., Bhave, P.V., Divita, F., Hsu, Y., Luecken, D., Mobley, J.D., Pouliot, G.A., Reff, A.,
41 Sarwar, G., and Strum, M.: The development and uses of EPA's SPECIATE database. *Atmospheric*
42 *Pollution Research*, 1(4) 196-206, 2010.

- 1 Skamarock, W.C., Klemp, J.B., Dudhia, J., Gill, D.O., Barker, D.M., Duda, M.G., Huang, X.Y., Wang, W.,
2 and Powers, J.G.: A Description of the Advanced Research WRF Version 3. NCAR, NCAR Technical Note
3 NCAR/TN-475+STR, DOI: 10.5065/D68S4MVH, 2008.
- 4 Sun, Y. L., Zhuang, G. S., Wang, Y., Zhao, X. J., Li, J., Wang, Z. F., and An, Z. S.: Chemical composition
5 of dust storms in Beijing and implications for the mixing of mineral aerosol with pollution aerosol on the
6 pathway, *Journal of Geophysical Research-Atmospheres*, 110, D24209, doi:10.1029/2005JD006054, 2005.
- 7 Tang, Y. H., Carmichael, G. R., Kurata, G., Uno, I., Weber, R. J., Song, C. H., Guttikunda, S. K., Woo, J.
8 H., Streets, D. G., Wei, C., Clarke, A. D., Huebert, B., and Anderson, T. L.: Impacts of dust on regional
9 tropospheric chemistry during the ACE-Asia experiment: A model study with observations, *Journal of*
10 *Geophysical Research-Atmospheres*, 109, D19S21, doi:10.1029/2003JD003806, 2004.
- 11 Tatarov, B., Muller, D., Noh, Y. M., Lee, K. H., Shin, D. H., Shin, S. K., Sugimoto, N., Seifert, P., and Kim,
12 Y. J.: Record heavy mineral dust outbreaks over Korea in 2010: Two cases observed with multiwavelength
13 aerosol/depolarization/Raman-quartz lidar, *Geophysical Research Letters*, 39, L14801,
14 doi:10.1029/2012GL051972, 2012.
- 15 Tsai, F. J., Fang, Y. S., and Huang, S. J.: Case Study of Asian Dust Event on March 19-25, 2010 and Its
16 Impact on the Marginal Sea of China, *Journal of Marine Science and Technology-Taiwan*, 21, 353-360,
17 2013.
- 18 Tong, D. Q., Bowker, G. E., He, S., Byun, D. W., Mathur, R., and Gillette, D. A.: Development of a
19 windblown dust emission model FENGSHAA description and initial application in the United States, In
20 review, 2016.
- 21 Uno, I., Amano, H., Emori, S., Kinoshita, K., Matsui, I., and Sugimoto, N.: Trans-Pacific yellow sand
22 transport observed in April 1998: A numerical simulation, *Journal of Geophysical Research-Atmospheres*,
23 106, 18331-18344, 2001.
- 24 Usher, C. R., Michel, A. E., and Grassian, V. H.: Reactions on mineral dust, *Chemical Reviews*, 103,
25 4883-4939, 2003.
- 26 Vogel, B., Vogel, H., Kleffmann, J., and Kurtenbach, R.: Measured and simulated vertical profiles of
27 nitrous acid - Part II. Model simulations and indications for a photolytic source, *Atmospheric Environment*,
28 37, 2957-2966, 2003.
- 29 Wang, K., Zhang, Y., Nenes, A., and Fountoukis, C.: Implementation of dust emission and chemistry into
30 the Community Multiscale Air Quality modeling system and initial application to an Asian dust storm
31 episode, *Atmospheric Chemistry and Physics*, 12, 10209-10237, [doi:10.5194/acp-12-10209-2012](https://doi.org/10.5194/acp-12-10209-2012), 2012.
- 32 Wang, S. X., Xing, J., Chatani, S., Hao, J. M., Klimont, Z., Cofala, J., and Amann, M.: Verification of
33 anthropogenic emissions of China by satellite and ground observations, *Atmospheric Environment*, 45,
34 6347-6358, 2011.
- 35 Washington, R., Todd, M., Middleton, N. J., and Goudie, A. S.: Dust-storm source areas determined by the
36 total ozone monitoring spectrometer and surface observations, *Annals of the Association of American*
37 *Geographers*, 93, 297-313, 2003.
- 38 Xing, J., Mathur, R., Pleim, J., Hogrefe, C., Gan, C.-M., Wong, D. C., Wei, C., Gilliam, R., and Pouliot, G.:
39 Observations and modeling of air quality trends over 1990–2010 across the Northern Hemisphere: China,
40 the United States and Europe. *Atmospheric Chemistry and Physics*, 15, 2723–2747, 2015.
- 41 Yarwood, J., Rao, S., Yocke, Ma., Whitten, G.Z., and Reyes, S.: Updates to the Carbon Bond Mechanism:
42 CB05, Final Report to the US EPA, RT-0400675, Chapel Hill, NC, December, 2005.

- 1 Zhang, X. Y., Gong, S. L., Zhao, T. L., Arimoto, R., Wang, Y. Q., and Zhou, Z. J.: Sources of Asian dust
2 and role of climate change versus desertification in Asian dust emission, *Geophysical Research Letters*, 30,
3 2272, doi:10.1029/2003GL018206, 2003.
- 4 Zhao, B., Wang, S. X., Dong, X. Y., Wang, J. D., Duan, L., Fu, X., Hao, J. M., and Fu, J.: Environmental
5 effects of the recent emission changes in China: Implications for particulate matter pollution and soil
6 acidification, *Environmental Research Letters*, 8, 024031, doi:10.1088/1748-9326/8/2/024031, 2013.
- 7 Zhao, C., Liu, X., Leung, L. R., Johnson, B., McFarlane, S. A., Gustafson, W. I., Fast, J. D., and Easter, R.:
8 The spatial distribution of mineral dust and its shortwave radiative forcing over North Africa: Modeling
9 sensitivities to dust emissions and aerosol size treatments, *Atmospheric Chemistry and Physics*, 10,
10 8821-8838, 2010.
- 11 Zhu, H. and Zhang, H. S.: An estimation of the threshold friction velocities over the three different dust
12 storm source areas in northwest China (in Chinese), *Acta. Meteorol. Sin.*, 68, 977–984, 2010.
- 13 Zhuang, G. S., Yi, Z., Duce, R. A., and Brown, P. R.: Link between Iron and Sulfur Cycles Suggested by
14 Detection of Fe(II) in Remote Marine Aerosols, *Nature*, 355, 537-539, 1992.
- 15

1

Table 1. Value of the saturation soil moisture limit (S_f)

<u>Soil Type</u>	<u>Landcover</u>	<u>Shrubland</u>	<u>Mixed shrub/grass land</u>	<u>Barren or sparsely vegetated</u>
<u>Sand</u>		<u>0.395</u>	<u>0.135</u>	<u>0.068</u>
<u>Loamy sand</u>		<u>0.410</u>	<u>0.150</u>	<u>0.075</u>
<u>Sandy loam</u>		<u>0.435</u>	<u>0.195</u>	<u>0.114</u>
<u>Silt loam</u>		<u>0.485</u>	<u>0.255</u>	<u>0.179</u>
<u>Silt</u>		<u>0.476</u>	<u>0.361</u>	<u>0.084</u>
<u>Lam</u>		<u>0.451</u>	<u>0.240</u>	<u>0.155</u>
<u>Sandy clay loam</u>		<u>0.420</u>	<u>0.255</u>	<u>0.175</u>
<u>Silty clay loam</u>		<u>0.477</u>	<u>0.322</u>	<u>0.218</u>
<u>Clay loam</u>		<u>0.476</u>	<u>0.325</u>	<u>0.250</u>
<u>Sandy clay</u>		<u>0.426</u>	<u>0.310</u>	<u>0.219</u>
<u>Silty clay</u>		<u>0.482</u>	<u>0.370</u>	<u>0.283</u>
<u>Clay</u>		<u>0.482</u>	<u>0.367</u>	<u>0.286</u>

2

1 Table 12. Dust emission speciation profiles from the default CMAQ, and the profiles
2 derived in this study for the Taklamakan and Gobi deserts. ~~Simulation results of ACA,~~
3 ~~AMG, and AK (in bold) will be evaluated against observations in next section.~~

Model Species	Description	Mass Contributions (%)					
		Fine Mode (I,J mode in CMAQ $\leq 2.5\mu\text{m}$)			Coarse Mode (K mode in CMAQ $\leq 10\mu\text{m}$)		
		Default	Taklamakan	Gobi	Default	Taklamakan	Gobi
ASO4	Sulfate (SO_4^{2-})	2.5	3.554	0.953	2.655	2.825	0.471
ANO3	Nitrate (NO_3^-)	0.02	0.181	0.204	0.16	0.125	0.084
ACL	Chloride (Cl^-)	0.945	2.419	0.544	1.19	2.357	0.094
ANH4	Ammonium (NH_4^+)	0.005	0.098	0.346	0	0.066	0.185
ANA	Sodium (Na^+)	3.935	2.234	1.016	0	2.056	0.301
ACA	Calcium (Ca_2^+)	7.94	2.063	1.788	0	1.423	1.082
AMG	Magnesium (Mg_2^+)	0	0.165	0.799	0	0.121	0.819
AK	Potassium (K^+)	3.77	0.153	0.282	0	0.108	0.121
Primary Organic							
APOC	Carbon	1.075	1.075	1.075	0	0	0
Non-carbon organic							
APNCOM	matter	0.43	0.43	0.43	0	0	0
AEC	Elementary carbon	0	0	0	0	0	0
AFE	Iron (Fe)	3.355	4.689	2.425	0	3.75	3.055
AAL	Aluminum (Al)	5.695	5.926	4.265	0	4.987	4.641
ASI	Silicon (Si)	19.425	20.739	14.929	0	17.454	16.245
ATI	Titanium (Ti)	0.28	0.312	0.337	0	0.285	0.365
AMN	Manganese (Mn)	0.115	0.0758	0.063	0	0.062	0.072

AH2O	Water (H_2O)	0.541	0.541	0.541	0	0	0
AOTHR	Unspeciated	50.219	55.345	70.002	0	0	0
ASOIL	Non-anion dust	0	0	0	95.995	64.382	72.464

1

2

1 Table 23. Heterogeneous reactions and uptake coefficients

No.	Reaction	Uptake coefficient	References
Default heterogeneous reactions in CMAQv5.0.1			
C1	$N_2O_5 + H_2O \longrightarrow 2HNO_3$	$\gamma = \begin{cases} (x_1 + x_2) \times \gamma_d^* + x_3 \times \min(\gamma_d^*, \gamma_3), & RH < CRH \\ \sum_{i=1}^3 x_i \times \gamma_i^*, & RH > IRH \\ 0.02, & otherwise \end{cases}$ <p>where x_1, x_2, x_3 and $\gamma_1, \gamma_2, \gamma_3$ are the normalized molar concentrations and N_2O_5 uptake coefficients on NH_4HSO_4, $(NH_4)_2SO_4$, and NH_4NO_3 respectively, $\gamma_d^* = \min(\gamma_d, 0.0124)$ where γ_d is the uptake coefficient on dry particles determined by relative humidity and temperature, RH is relative humidity, CRH is crystallization relative humidity, IRH is ice formation relative humidity determined by temperature</p>	Davis et al. (2008)
C2	$2NO_2 + H_2O \longrightarrow HONO + HNO_3$	$K = 5.0 \times 10^{-6} \times A_p$	Vogel et al. (2003)
Implemented dust heterogeneous reactions in this work			
R1	$O_3 + dust \longrightarrow products$	$5.0 \times 10^{-5} \sim 1.0 \times 10^{-4}$	Zhu et al. (2010)
R2	$OH + dust \longrightarrow products$	$0.1 \sim 1.0$	Zhu et al. (2010)
R3	$H_2O_2 + dust \longrightarrow products$	$1.0 \times 10^{-4} \sim 2.0 \times 10^{-3}$	Zhu et al. (2010)
R4	$CH_3COOH + dust \longrightarrow products$	1.0×10^{-3}	Zhu et al. (2010)
R5	$CH_3OH + dust \longrightarrow products$	1.0×10^{-5}	Zhu et al. (2010)

R6	$CH_2O + dust \longrightarrow products$	1.0×10^{-5}	Zhu et al. (2010)
R7	$HNO_3 + dust \longrightarrow 0.5NO_3^- + 0.5NO_x$	$1.1 \times 10^{-3} \sim 0.2$	Dentener et al. (1996)
R8	$N_2O_5 + dust \longrightarrow 2NO_3^-$	$1 \times 10^{-3} \sim 0.1$	Zhu et al. (2010)
R9	$NO_2 + dust \longrightarrow NO_3^-$	$4.4 \times 10^{-5} \sim 2.0 \times 10^{-4}$	Underwood et al. (2001)
R10	$NO_3 + dust \longrightarrow NO_3^-$	$0.1 \sim 0.23$	Underwood et al. (2001)
R11	$NO_3 + dust \longrightarrow HNO_3$	1.0×10^{-3}	Martin et al. (2003)
R12	$HO_2 + dust \longrightarrow 0.5H_2O_2$	0.2	Zhu et al. (2010)
R13	$SO_2 + dust \longrightarrow SO_4^{2-}$	$1.0 \times 10^{-4} \sim 2.6 \times 10^{-4}$	Padnis and Carmichael (2000)

1

2

1 Table 34. Simulation Design

Scenario	Configuration of CMAQv5.0.1
Dust_Off	Without inline calculation of dust
Dust_Default	With default dust plume rise scheme
Dust_Revised	Revised initial friction velocity threshold constant in dust plume rise scheme
Dust_Profile	Same as Dust_Revised, but with implemented source-dependent speciation profile
Dust_Chem	Same as Dust_Profile, but with implemented dust chemistry with lower limit of uptake coefficient
Dust_ChemHigh	Same as Dust_Chem, but with upper limit of uptake coefficients

2

3

Dataset	Species measured	Observational frequency	Number of sites	Data source
AERONET	AOD	Daily	70 sites within our simulation domain	http://aeronet.gsfc.nasa.gov/cgi-bin/combined_data_access_new
API	PM ₁₀	Daily	86 cities in China	http://datacenter.mep.gov.cn
EANET	PM ₁₀ , SO ₂ , NO _x , HNO ₃ , O ₃	Hourly/Daily/Bi-weekly	11 sites in Japan	http://www.eanet.asia/
Fudan Univ. Obs	K^+ , Mg_2^+ , Ca_2^+ , PM _{2.5}	Daily (2007 only)	Duolun (42.18°N, 116.48°E), Yulin (38.3°N, 109.77°E)	Huang et al. (2010)
MODIS	AOD	Daily	-	http://ladsweb.nascom.nasa.gov/data/search.html
TAQMN	PM ₁₀	Daily	Xinzhuang (25.03°N, 121.43°E)	http://taqm.epa.gov.tw/taqm/en/default.aspx

		Table 56. Evaluation statistics for tracer metals and PM _{2.5}						
		PM _{2.5}	<i>K</i> ⁺		<i>Mg</i> ₂ ⁺		<i>Ca</i> ₂ ⁺	
			Dust_Revised	Dust_Profile	Dust_Revised	Dust_Profile	Dust_Revised	Dust_Profile
Mean	Obs	81.52	0.23		0.19		2.24	
(μg/m ³)								
Mean	Sim	44.36	0.69	0.12	0.02	0.12	3.06	1.05
(μg/m ³)								
MB (μg/m ³)		-37.17	0.46	-0.11	-0.17	-0.07	0.82	-1.19
NMB (%)		-45.59	208.9	-47.83	-99.8	-36.84	36.69	-53.12
R		0.67	0.42	0.44	0.22	0.51	0.22	0.44

2

3

1 Table 67. CMAQ evaluation against EANET observations for Dust_Profile, Dust_Chem,
2 and Dust_ChemHigh scenarios for species O₃, SO₂, SO₄²⁻, NO_x, HNO₃, and NO₃⁻

		O ₃ (ppbv)	SO ₂ (ppbv)	SO ₄ ²⁻ (µg/m ³)	NO _x (ppbv)	HNO ₃ (ppbv)	NO ₃ ⁻ (µg/m ³)
Mean Obs		45.81	0.59	4.38	1.75	0.43	1.52
MB	Dust_Profile	0.59	0.54	-0.71	0.63	0.46	-0.20
	Dust_Chem	-0.92	0.42	0.60	0.67	0.36	-0.03
	Dust_ChemHigh	-2.07	0.38	1.29	0.68	0.35	0.37
NMB (%)	Dust_Profile	1.26	90.70	-16.28	35.61	109.03	-13.07
	Dust_Chem	-1.97	69.83	13.74	37.79	85.17	-1.97
	Dust_ChemHigh	-4.43	63.70	29.43	38.21	81.24	24.09
R	Dust_Profile	0.63	0.68	0.79	0.69	0.65	0.71
	Dust_Chem	0.62	0.65	0.75	0.69	0.59	0.72
	Dust_ChemHigh	0.59	0.64	0.72	0.69	0.60	0.73

3

4

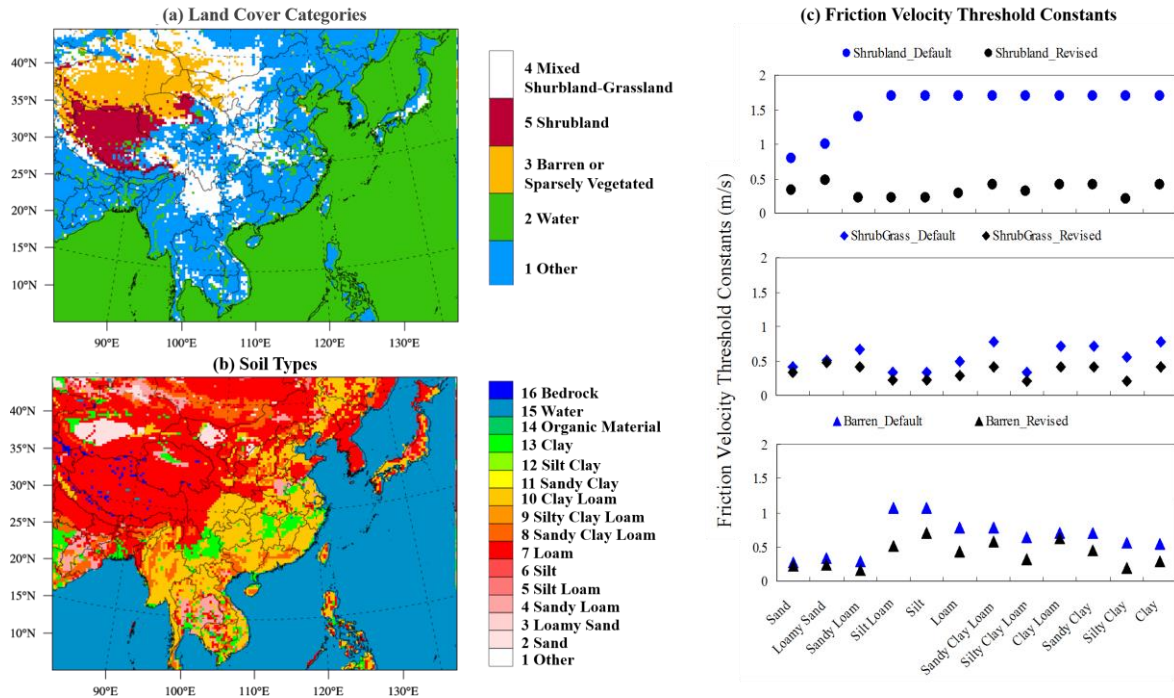


Figure 1. (a) Land cover categories, (b) Soil types, and (c) comparison of initial friction velocity threshold constants in default (blue markers) and revised (black markers) dust schemes for shrub land (top), mixed shrub and grassland (middle), and barren or sparsely vegetated (bottom) land cover.

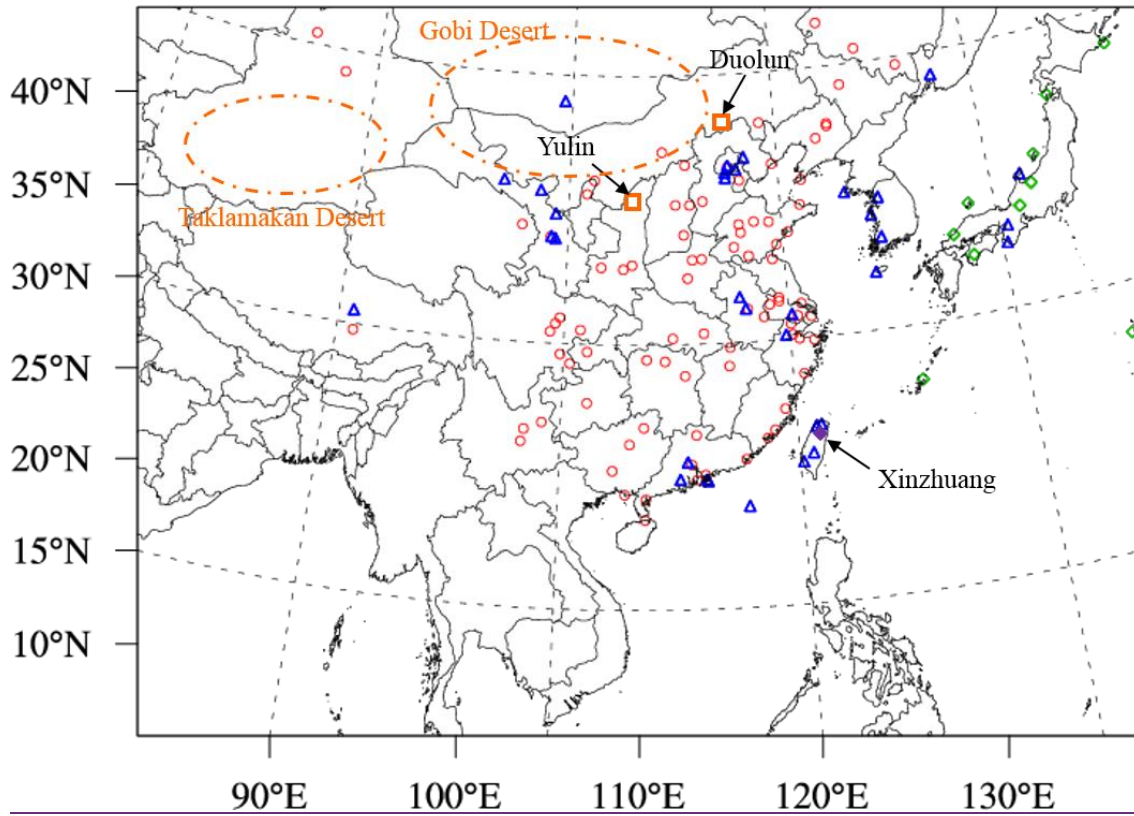
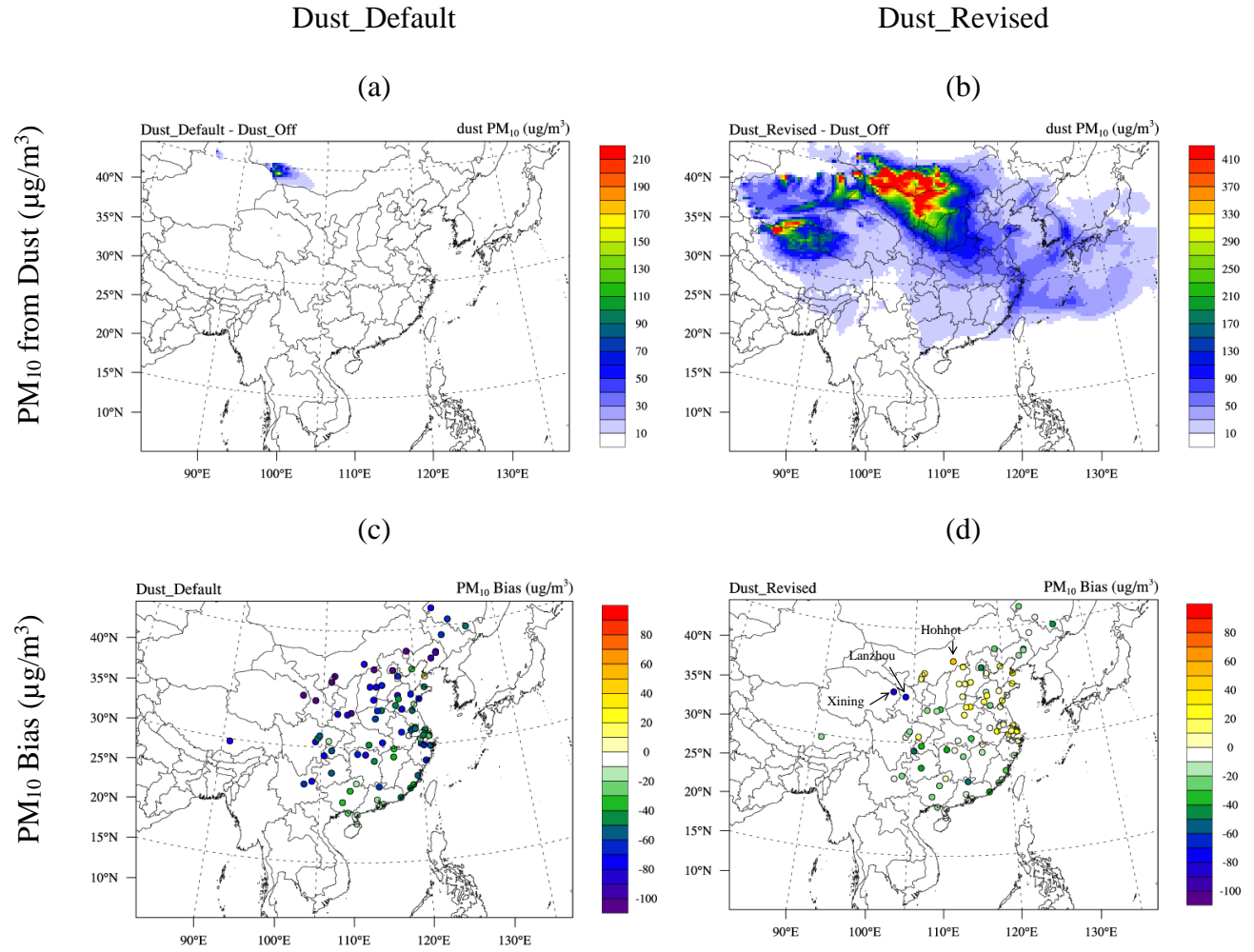


Figure 2. Modeling domain and locations of observation stations from Fudan observation network (orange rectangles), API (red circles), AERONET (blue triangles), EANET (green diamonds), and TAQMN (purple diamonds) over East Asia.

1

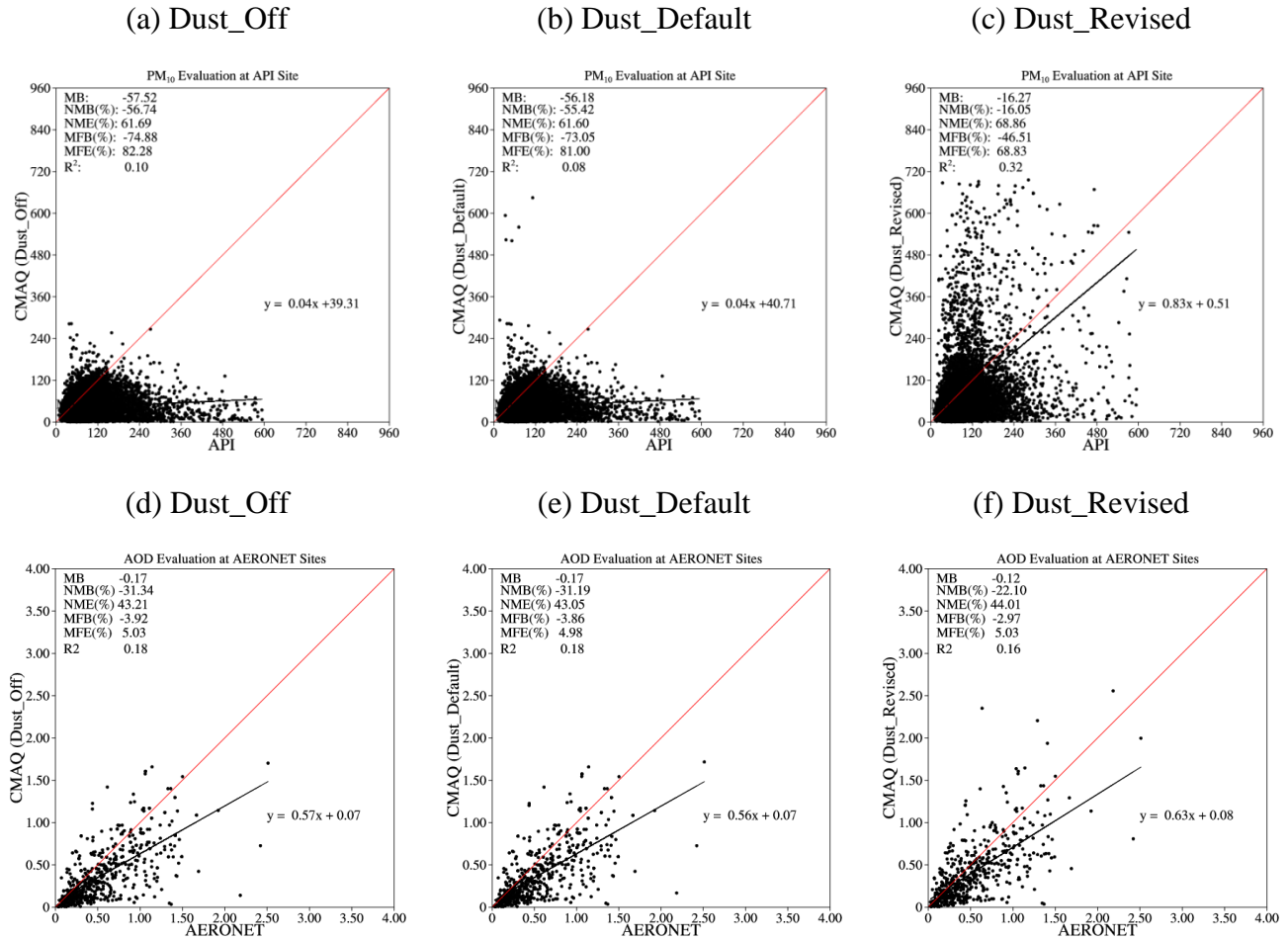


2

3 Figure 3. Five-years averages of PM₁₀ concentration difference from (a) Dust_Default -
 4 Dust_Off, and (b) Dust_Revised - Dust_Off. PM₁₀ simulation bias against observation at
 5 API stations for (c) Dust_Default and (d) Dust_Revised scenarios.

6

1

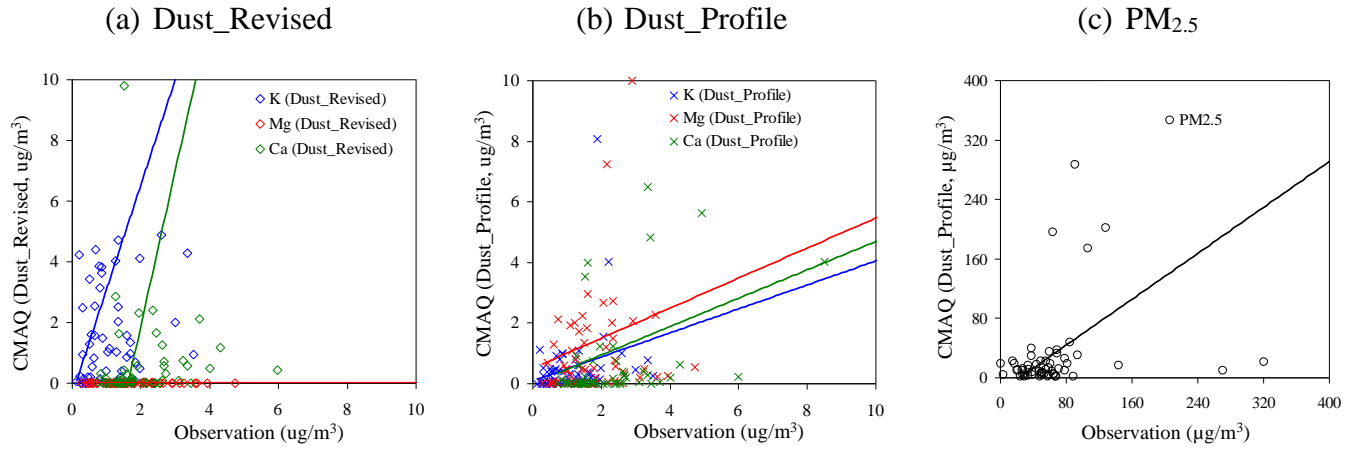


2

3 Figure 4. CMAQ evaluation against PM₁₀ from API (upper row) and AOD (bottom row)
 4 from AERONET for Dust_Off (left column), Dust_Default (middle column), and
 5 Dust_Revised (right column) scenarios. Formula of calculating evaluation statistics
 6 including mean bias (MB), normalized mean bias (NMB), normalized mean error (NME),
 7 mean fractional bias (MFB), mean fractional error (MFE), and correlation coefficient (R)
 8 can be found in Dong et al. (2013).

9

1



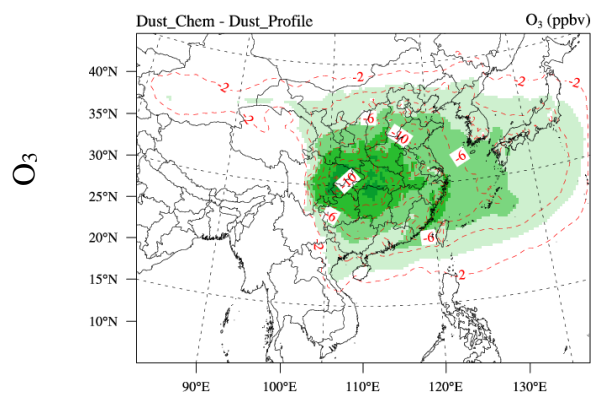
2

3 Figure 5. Model evaluations of CMAQ simulated metal tracers against observations from
 4 Fudan University ([shown in Table 5](#)) at Duolun and Yulin for (a) Dust_Revised and (b)
 5 Dust_Profile scenarios. [Evaluation statistics are shown in Table 6](#). Note that simulations
 6 and observations of K^+ and Mg_2^+ are upscaled by 5 and 10 times, respectively, to
 7 make them comparable with Ca_2^+ in the same plot. Right column is the evaluation of
 8 CMAQ simulated (c) PM_{2.5} at Duolun and Yulin.

9

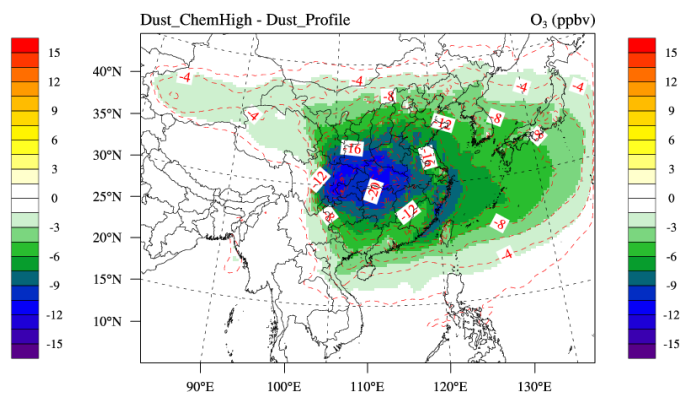
Dust_Chem - Dust_Revised

(a)

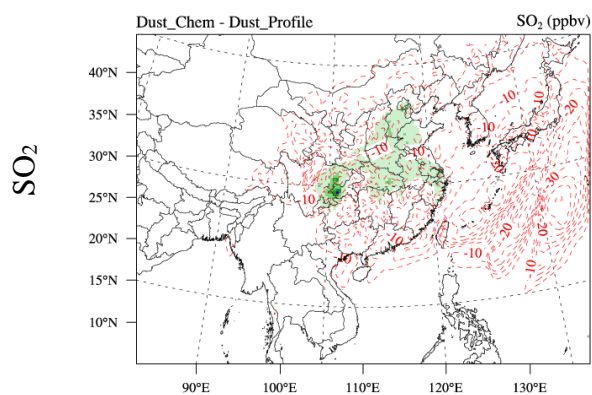


Dust_ChemHigh - Dust_Revised

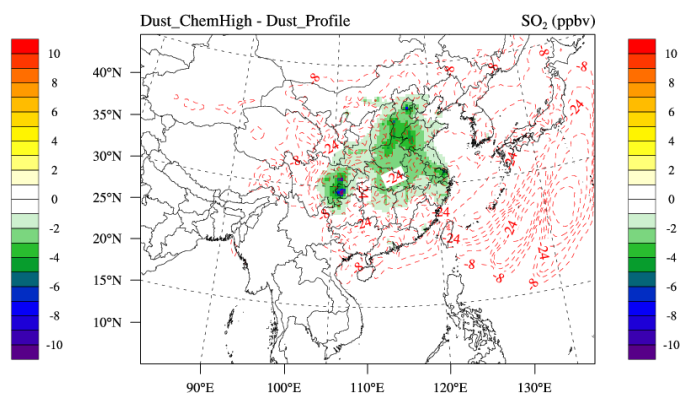
(b)



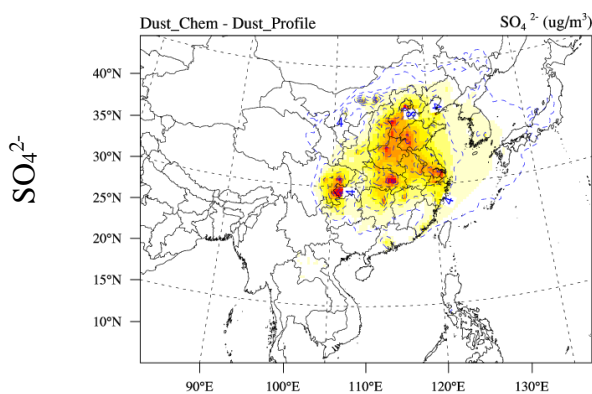
(c)



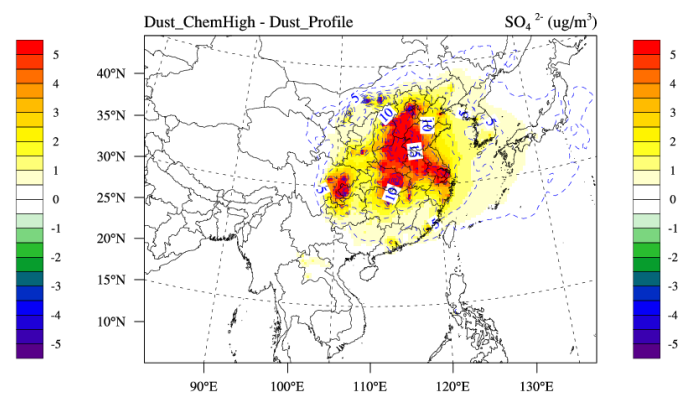
(d)

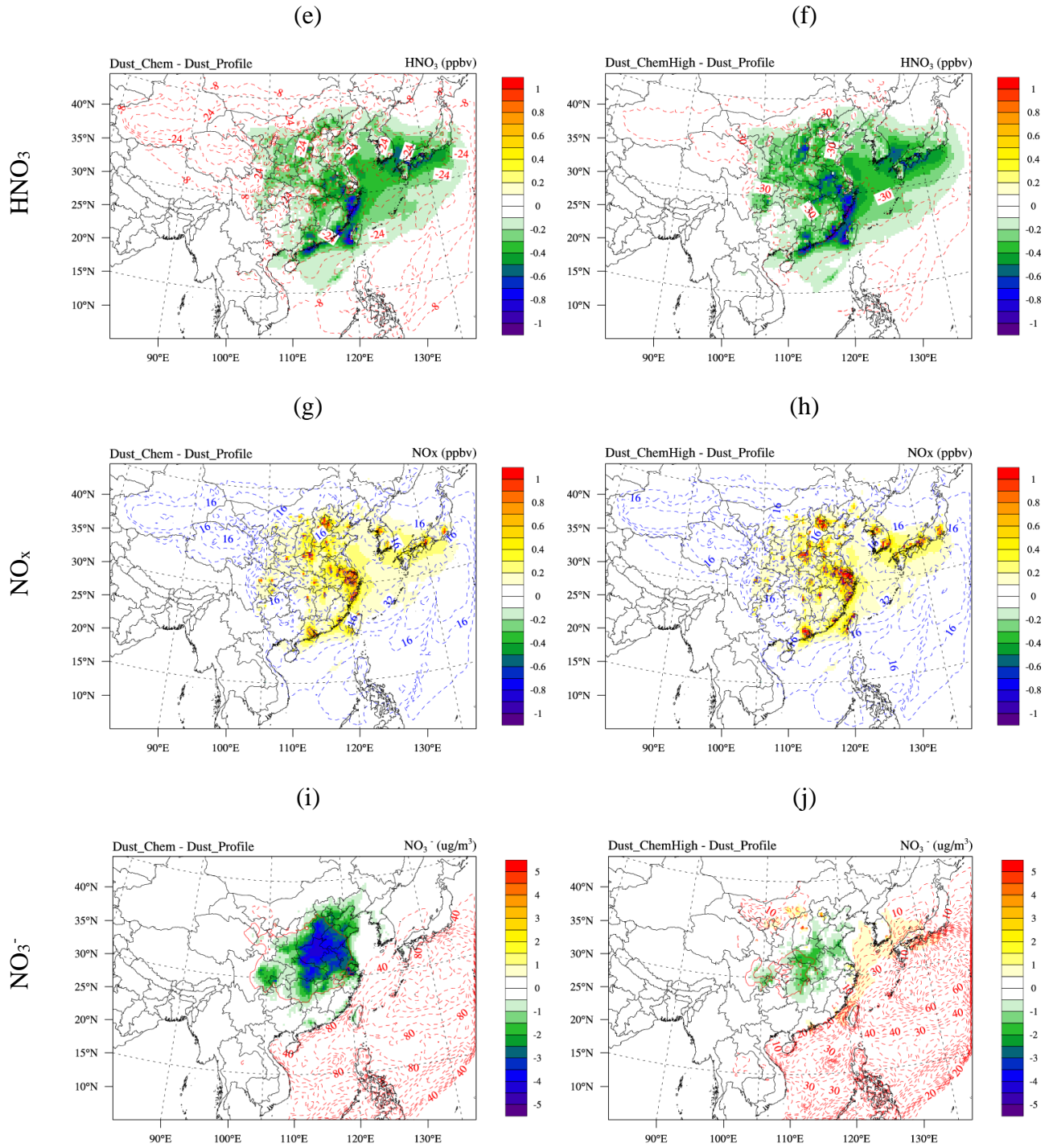


(c)



(d)

 SO_4^{2-}



1

2 Figure 6. Five-year averages for March and April from 2006 to 2010 of dust
 3 heterogeneous chemistry impacts with lower (left column) and upper (right column)
 4 uptake coefficients, for species O_3 (1st row), SO_2 (2nd row), SO_4^{2-} (3rd row), HNO_3 (4th row)

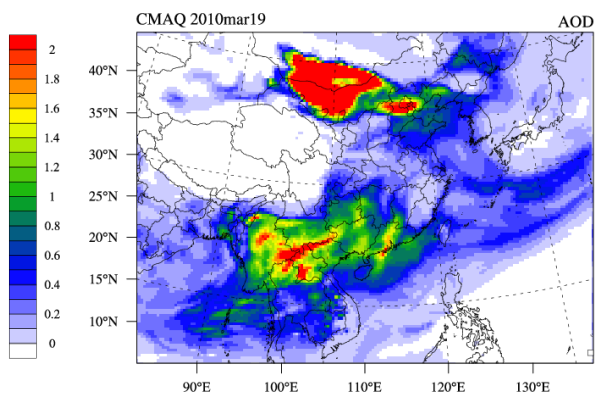
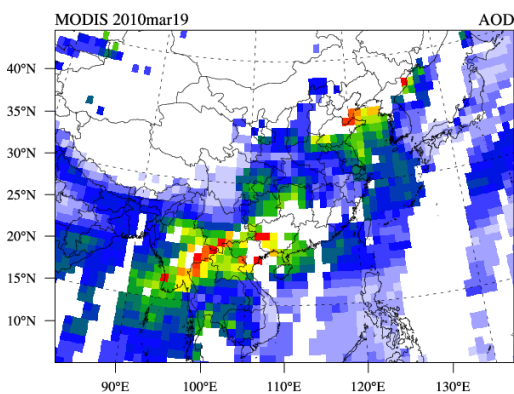
1 ~~row~~), NO_x (~~5th row~~), and NO_3^- (~~6th row~~). Color contours represent the absolute
2 concentration changes, and dash contour lines with numbers indicate the percentage
3 changes.
4

MODIS

CMAQ

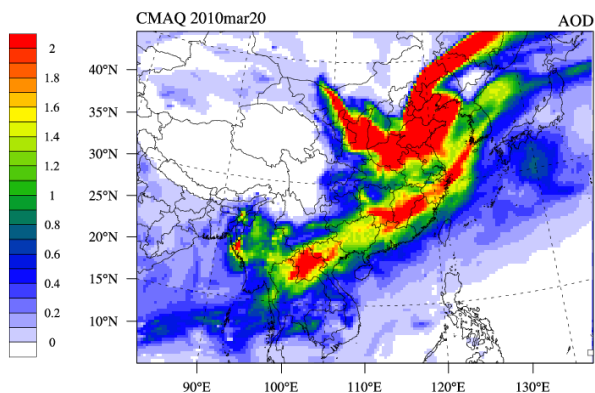
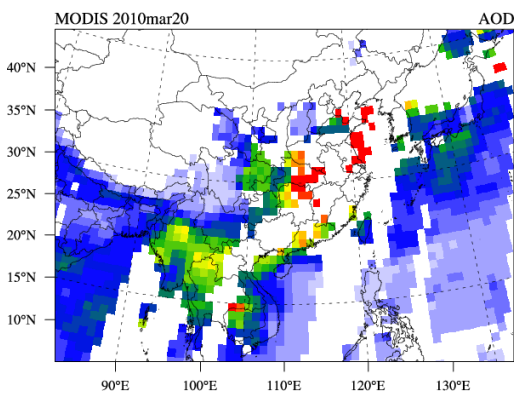
(a) Mar.19th 2010

(b) Mar.19th 2010



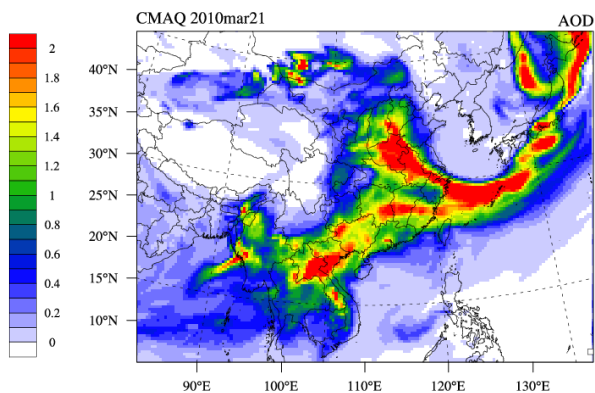
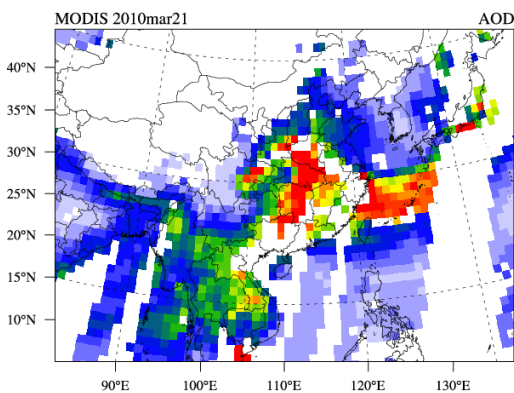
(c) Mar.20th 2010

(d) Mar.20th 2010



(e) Mar.21st 2010

(f) Mar.21st 2010



1 Figure 7. Daily MODIS observed (left column) and CMAQ simulated AOD (right
2 column) for March 19th (top row), March 20th (middle row), and March 21st (bottom
3 row).
4

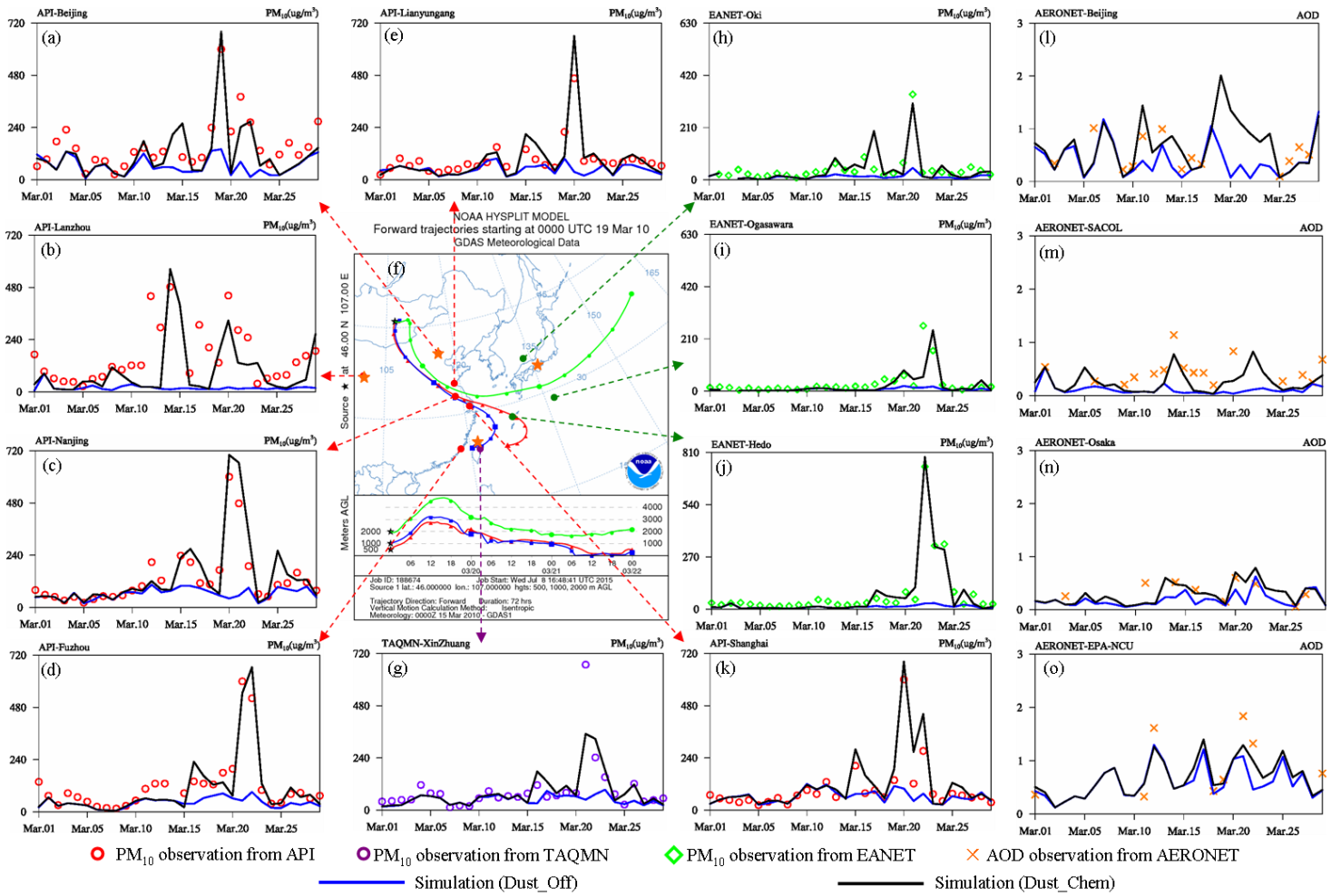


Figure 8. Forward trajectories from (f) HYSPLIT, and temporal variations of PM_{10} and AOD on a daily scale. Comparison between simulated (black lines for Dust_Chem scenario, and blue lines for Dust_Off scenario) and observed PM_{10} from API (red circles) at (a) Beijing, (b) Lanzhou, (c) Nanjing, (d) Xiamen, (e) Lianyungang, and (k) Shanghai. Comparison between simulations and observed PM_{10} from TAQMN (purple circles) at (g) Xinzhuang. Comparison between simulations and observed AOD from EANET (green diamonds) at (l) Beijing, (m) SACOL, (n) Osaka, and (o) NCU. Locations of cities or stations are indicated by the tails of arrow lines (for PM_{10}) or orange stars (for AOD)

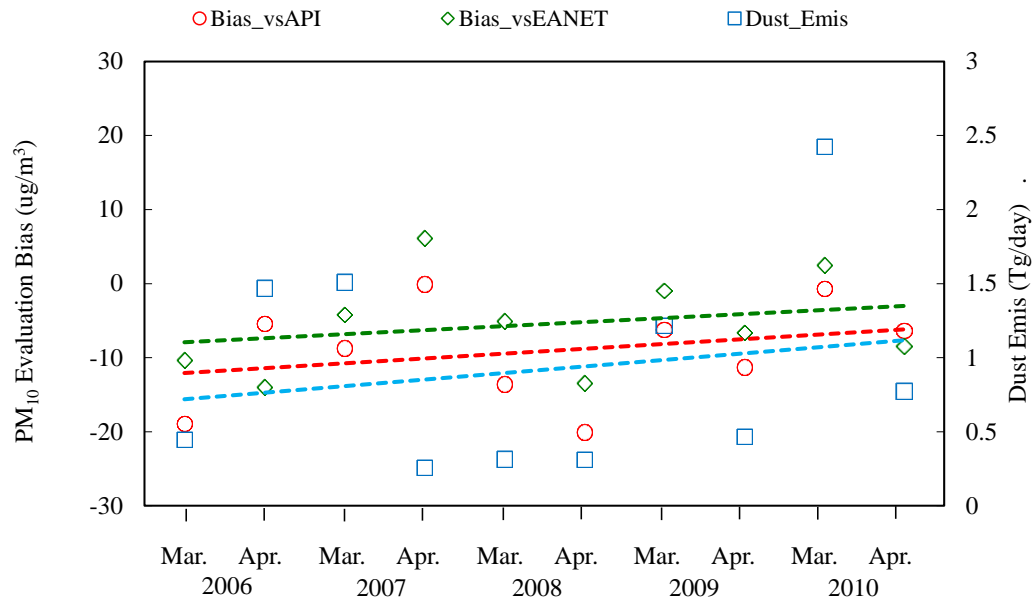
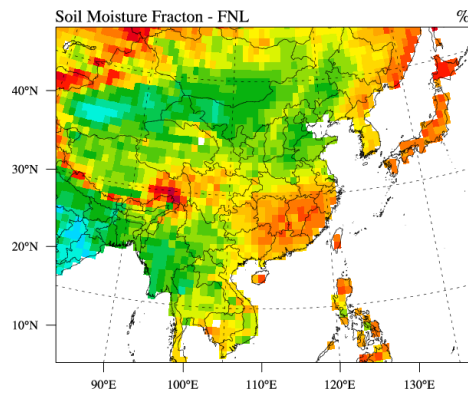


Figure 9. CMAQ predictions of dust emission rate (solid orange rectangles), and simulation bias of PM_{10} against observations from API (red circles) and EANET (green diamonds). Dash lines indicated the trends of the variables.

(a) FNL soil moisture fraction



(b) GLDAS soil moisture fraction

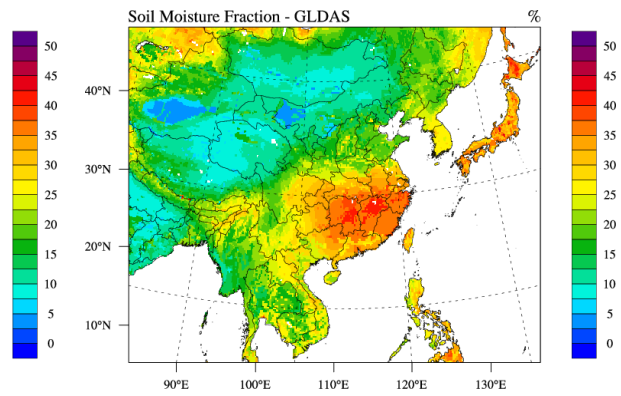


Figure 10. Five-year averages (for March and April) of soil moisture fraction in top 10cm soil depth from (a) FNL and (b) GLDAS.